



저작자표시-비영리-변경금지 2.0 대한민국

이용자는 아래의 조건을 따르는 경우에 한하여 자유롭게

- 이 저작물을 복제, 배포, 전송, 전시, 공연 및 방송할 수 있습니다.

다음과 같은 조건을 따라야 합니다:



저작자표시. 귀하는 원저작자를 표시하여야 합니다.



비영리. 귀하는 이 저작물을 영리 목적으로 이용할 수 없습니다.



변경금지. 귀하는 이 저작물을 개작, 변형 또는 가공할 수 없습니다.

- 귀하는, 이 저작물의 재이용이나 배포의 경우, 이 저작물에 적용된 이용허락조건을 명확하게 나타내어야 합니다.
- 저작권자로부터 별도의 허가를 받으면 이러한 조건들은 적용되지 않습니다.

저작권법에 따른 이용자의 권리는 위의 내용에 의하여 영향을 받지 않습니다.

이것은 [이용허락규약\(Legal Code\)](#)을 이해하기 쉽게 요약한 것입니다.

[Disclaimer](#)

Modulation of chemotherapy-induced
peripheral neuropathy by JZL195 through
glia and endocannabinoid system

Leejeong Kim

Department of Medical Science

The Graduate School, Yonsei University

Modulation of chemotherapy-induced
peripheral neuropathy by JZL195 through
glia and endocannabinoid system

Directed by Professor Bae Hwan Lee

The Master's Thesis
submitted to the Department of Medical Science,
the Graduate School of Yonsei University
in partial fulfillment of the requirements for the degree of
Master of Medical Science

Leejeong Kim

December 2023

This certifies that the Master's Thesis
of Leejeong Kim is approved.

Thesis Supervisor : Bae Hwan Lee

Thesis Committee Member #1 : Sun Joon Bai

Thesis Committee Member #2 : Kyung Hee Lee

The Graduate School
Yonsei University

December 2023

TABLE OF CONTENTS

ABSTRACT.....	v
I. INTRODUCTION	1
II. MATERIALS AND METHODS	5
1. Experimental animal	5
2. Experimental designs	5
3. Drugs	7
4. Chemotherapy-induced peripheral neuropathy model	8
5. JZL195, AM251 and AM630 injections	8
6. Behavioral tests	9
A. Mechanical allodynia assessment	9
B. Cold allodynia assessment	9
C. Open field test	10
7. Western blot analysis	10
8. Immunohistochemistry staining	11
9. Statistical analysis	12
III. RESULTS	13
1. Differences in locomotor behaviors on day 8 and day 15 in the CIPN animal model	13
2. JZL195 alleviates mechanical and cold allodynia in an animal model of CIPN	17
3. JZL195 with locomotor activity in the CIPN animal model	20
4. JZL195 inhibited FAAH/MAGL and regulated the cannabinoid receptors differently in the DRG and spinal cord	25
5. FAAH/MAGL inhibition decreased the TLR4 and pro-inflammatory	

factors in the DRG and spinal cord	28
6. The regulation of glial cell activation in the DRG and spinal cord after FAAH/MAGL inhibition	30
7. Satellite cells in the DRG are regulated by JZL195, along with CB1R, CB2R, and TLR4 expression	33
8. CB1R, CB2R, and TLR4 co-localized with astrocytes in the spinal cord	38
9. CB1R, CB2R, and TLR4 co-localized with microglia in the spinal cord	44
10. Two types of cannabinoid receptors act similarly on pain-relief effects	48
11. JZL195 did not affect locomotor activity as well as pain-related behavior in normal mice	51
IV. DISCUSSION	55
1. The animal model of CIPN exhibits different locomotor activities depending on the development stage	55
2. Inhibition of FAAH/MAGL alleviates chemotherapy-induced peripheral neuropathy	57
3. The ECS in the DRG and spinal cord of the CIPN animal model is differentially regulated	58
4. CIPN can be alleviated through TLR4 in spinal astrocytes and microglia by modulating CB1R and CB2R	61
5. Antinociceptive effects of JZL195 were mediated by spinal cannabinoid receptors	62
V. CONCLUSION	65
REFERENCES	66
ABSTRACT (IN KOREAN)	76

LIST OF FIGURES

Figure 1. An illustration of overall experimental design	7
Figure 2. Assessment of the mechanical allodynia, cold allodynia, and locomotor activity of the mice after cisplatin injection ...	15
Figure 3. Assessment of the mechanical allodynia, cold allodynia, and body weight in CIPN animal model after JZL195 administration	19
Figure 4. Assessments of locomotor activities of the CIPN mice after JZL195 administration on day 15	23
Figure 5. The representative western blot images and quantification of FAAH, MAGL, CB1R, and CB2R expression level in the L4-L6 DRG and spinal cord	26
Figure 6. The representative western blot images and quantification of TLR4, TNF- α , and IL-1 β expression level in the L4-L6 DRG and spinal cord	29
Figure 7. The representative western blot images and quantification of GFAP and Iba1 level in the L4-L6 DRG and spinal cord	32
Figure 8. Expression of satellite glial cells with CB1R, CB2R, and TLR4	35
Figure 9. Co-localization of CB1R, CB2R, and TLR4 expression with astrocytes	40
Figure 10. Co-localization of CB1R, CB2R, and TLR4 expression	

with microglia	45
Figure 11. Assessment of the mechanical allodynia and cold allodynia after administrating antagonists for cannabinoid receptors	50
Figure 12. Effect of the JZL195 on locomotor activity and withdrawal thresholds in normal mice	53

ABSTRACT

Modulation of chemotherapy-induced peripheral neuropathy by JZL195 through glia and endocannabinoid system

Leejeong Kim

*Department of Medical Science
The Graduate School, Yonsei University*

(Directed by Professor Bae Hwan Lee)

Chemotherapy-induced peripheral neuropathy (CIPN) is one of the most serious side effects of chemotherapy. The pathophysiology of CIPN is complex and multifactorial, thereby its pathogenesis depends on the types of chemotherapy used. As a results, the clear mechanism behind CIPN remains elusive. However, recent attention has been given to neuroinflammation, which is modulated by the endocannabinoid system (ECS) and associated with glial activation, as a significant factor in the pathogenesis of CIPN. Therefore, the aim of this study was to investigate the pain-relieving effect of JZL195, which simultaneously inhibits fatty acid amide hydrolase (FAAH) and monoacylglycerol lipase (MAGL), in an animal model of CIPN and to investigate the correlation between the ECS and glial cells.

In this study, cisplatin was used to develop an animal model of CIPN. T hree different concentrations of JZL195 were then administered to the CIPN animal model. Both the up-down test and acetone test were conducted to assess mechanical and cold allodynia after JZL195 injections. Furthermore, western blot analysis was conducted to investigate the expression levels of the ECS and toll-like receptor 4 (TLR4), as well as the activation of glial cells, in the dorsal root ganglia (DRG) and

spinal cord. Immunohistochemistry staining was performed to determine whether the cannabinoid receptor 1/2 (CB1R and CB2R) and TLR4, which showed expressional changes in the DRG and spinal cord, were regulated by JZL195 within glial cells.

The results of behavioral analyses showed that 20 mg/kg of JZL195 provided significant pain relief for both mechanical and cold allodynia. Furthermore, the western blot analysis revealed distinct regulation of FAAH, MAGL, CB1R, and CB2R expression in the DRG and spinal cord. Additionally, treatment with JZL195 resulted in a reduction in the expression levels of TLR4, as well as TNF- α and IL-1 β , indicating that JZL195 might alleviate neuroinflammation. Furthermore, JZL195 inhibited the activation of satellite glial cells in the DRG, as well as astrocytes and microglia in the spinal cord, which were initially activated by cisplatin. Immunohistochemistry staining revealed changes in the morphology of glial cells, as well as alterations in the expression of CB1R, CB2R, and TLR4, which co-localized with astrocytes and microglia, but not with satellite glial cells.

These findings suggest that the inhibition of FAAH/MAGL with JZL195 can effectively alleviate CIPN and that the alleviation of CIPN is mediated through the close interaction between glial cell activity and cannabinoid receptors.

Key words: chemotherapy-induced peripheral neuropathy, endocannabinoid system, glia, neuroinflammation, toll-like receptor 4

Modulation of chemotherapy-induced peripheral neuropathy by JZL195 through glia and endocannabinoid system

Leejeong Kim

*Department of Medical Science
The Graduate School, Yonsei University*

(Directed by Professor Bae Hwan Lee)

I. INTRODUCTION

Chemotherapy-induced peripheral neuropathy (CIPN) is one of the most serious and dose-limiting side effects of chemotherapy.^{1,2} Approximately 30% of chemotherapy patients experiences CIPN.^{1,2} CIPN typically affects the peripheral areas of the body, particularly the hands and feet, and is characterized by a distribution pattern known as “glove and stocking”.³ The symptoms include numbness, paresthesia, dysesthesia, hyperalgesia, and allodynia, which can lead to chronic pain.³ These symptoms appear and persist during chemotherapy, often resulting in a reduction or premature cessation of treatment.⁴ Besides, CIPN can persist or worsen even after chemotherapy is discontinued, significantly impacting the overall quality of life for cancer patients.⁵⁻⁷ The pathophysiology of CIPN is complex and multifactorial, with the specific mechanisms depending on the type of chemotherapy used (*e.g.*, platinum drugs, taxanes, vinca alkaloids, bortezomib, and thalidomide).^{2,4} As a result, the exact mechanism underlying CIPN remains elusive. Recent research suggest that neuroinflammation plays a crucial role in CIPN.⁷⁻⁹ However, since there are currently no established preventative or therapeutic treatments for CIPN,^{1,7} understanding and modulating neuroinflammation is essential to

identify new targets for alleviating this condition.

Neuroinflammation is a localized inflammatory response in the central nervous system (CNS) and peripheral nervous system (PNS), characterized by increased production of pro-inflammatory substances and the activation of glial cells.^{10,11} There are growing evidences that chemotherapeutic agents can induce glial cell activation in both the CNS and PNS.¹²⁻¹⁶ In addition to controlling neuroinflammation, glial cells also contribute to pain.^{12,17-19} Given the profound role of glial cells in neuroinflammation and pain, numerous researchers have sought to alleviate CIPN by regulating glial cell activity. In a study on CIPN, microglia in the spinal cord were activated not only during cisplatin administration but also remained active even after the cessation of cisplatin exposure.²⁰ The activation of microglia was significantly reduced by minocycline, a microglial inhibitor, leading to pain relief.²⁰ In another study on CIPN, astrocytes showed significantly increased activation after paclitaxel administration in both male and female mice.¹⁴ Satellite glial cells (SGCs) in the PNS are also activated in response to noxious stimuli and pathological conditions, resulting in changes in their structure and the release of signaling molecules, such as pro-inflammatory cytokines and chemokines, which sensitize neurons and cause pain.^{6,14,15,19} In a study with using cultured satellite glial cells, the activation of glial fibrillary acidic protein (GFAP) progressively increased over time after cisplatin treatment.²¹ Furthermore, the release of TNF- α and IL-6 from SGCs was increased following cisplatin treatment.²¹ To date, various drugs and therapies have been used to alleviate CIPN by modulating glial cells.^{22,23} However, it remains unclear whether these approaches directly or indirectly influence glial activity in CIPN. Therefore, more specific mechanisms are needed to achieve better therapeutic effects with novel treatments.

Toll-like receptors (TLRs) are known to mediate neuroinflammation in infectious and non-infectious neurological diseases of the CNS.^{9,24} TLRs are pattern recognition receptors (PRRs) with a specific extracellular domain designed to recognize both pathogen-associated molecular patterns (PAMPs) and damage-associated molecular patterns (DAMPs).²⁵ TLRs contribute to the activation of the innate adaptive immune system and

are well-known for their role in inducing neuroimmune response by recognizing pathogens.^{9,26,27} TLRs are primarily expressed on glial cells, neurons, and immune cells in the CNS and PNS.^{25,26,28} Among the 13 subtypes of TLRs, TLR4 is one of the most widely characterized and plays a crucial role in the induction, conversion, and maintenance of chronic pain conditions.²⁵ Multiple recent studies have shown a significant correlation between TLR4 and neuropathic pain.²⁹⁻³¹ The underlying mechanism involves TLR4 triggering the activation of microglia and astrocytes, leading to the release of proinflammatory cytokines within the spinal cord.³² Consequently, this process contributes to the initiation and persistence of both inflammatory pain and neuropathic pain.³² Furthermore, TLR4 is known to play an important role in inflammatory responses and has been associated with neuroinflammation and neurotoxicity induced by chemotherapy.⁹ In a study on CIPN, the expression of TLR4 in the dorsal root ganglia (DRG) and spinal cord was increased by paclitaxel, while intrathecal administration of lipopolysaccharide derived from *R. sphaeroides* (LPS-RS), a TLR4 antagonist, prevented the development of CIPN.³³ Another study reported that intraperitoneal injections of cisplatin induced severe tactile allodynia with an increased dimerization of TLR4, the first step in the activation of a TLR4 inflammatory cascade, in spinal microglia.³⁴ Although studies on the TLR4 signaling pathway in CIPN are still lacking,⁹ as TLR4 is mainly expressed on microglia and astrocytes within the CNS and satellite glial cells of the PNS, modulation of TLR4 in glial cells may provide new insights to solve the unknown roles of the TLR4 signaling pathway and ultimately mitigate CIPN.

Endocannabinoids have attracted growing attention in CIPN pathogenesis due to their ability to modulate neuroinflammation, as well as their role in modifying pain perception.³⁵ The endocannabinoid system (ECS), which functions similarly to cannabis in the body,³⁶ plays an important role in pain control and immune-mediated inflammatory processes.³⁷⁻³⁹ The ECS is composed of cannabinoid receptors, endogenous cannabinoid ligands, endocannabinoids, and catabolic enzymes, namely fatty acid amide hydrolase (FAAH) and monoacylglycerol lipase (MAGL).⁴⁰ Cannabinoid receptors are G-protein-coupled

receptors, which are divided into cannabinoid receptor 1 (CB1R) and cannabinoid receptor 2 (CB2R).⁴⁰ CB1R is mainly expressed in the CNS, such as the brain and spinal cord, and plays a crucial role in pain transmission and regulation. CB2R, on the other hand, is mainly expressed in immune cells and glial cells, such as microglia and astrocytes. Anandamide (AEA) and 2-arachidonoylglycerol (2-AG), which are well-known endocannabinoids, are hydrolyzed by the catabolic enzymes FAAH and MAGL, respectively.^{41,42} As the ECS plays an important role in the neuropathic pain control and the chronicization of pain, previous studies have focused on pain control through treatments that act directly or indirectly on CB1R or CB2R.⁴³⁻⁴⁶ Recently, there have been attempts to modulate different types of pain using treatments that can act on both CB1R and CB2R with the expectation of synergistic effects. JZL195, a selective inhibitor of FAAH and MAGL, indirectly acts on the two major cannabinoid receptors, resulting in increased levels of the major endocannabinoids AEA and 2-AG.⁴⁷ JZL195 has demonstrated analgesic effects in neuropathic and inflammatory pain.^{48,49} A recent study reported that the dual FAAH/MAGL inhibitor JZL195 reduced inflammation-induced allodynia in the Complete Freund's Adjuvant model.

The studies on the pathogenesis of CIPN have been hindered by various factors that contribute to its development, leaving it as an unanswered question. Neuroinflammation, which has recently gained attention as a major factor in the pathogenesis of CIPN, is expected to make a significant contribution to understanding the mechanisms of CIPN. Therefore, the aim of the study was to investigate the pain-relieving effect of JZL195 by inhibiting FAAH/MAGL in a CIPN animal model. In addition, based on the aforementioned background, this study sought to provide insights into the potential connection between cannabinoid receptors and TLR4 in glial cells, which may be associated with neuroinflammation.

II. MATERIALS AND METHODS

1. Experimental animals

Male C57BL/6 mice (6 weeks old; 20–25 g; Orient Bio, Seongnam, Gyeonggi, South Korea) were utilized for the tests conducted in this study. The animals were housed in groups of five per cage and maintained under a 12-h light/12-h dark cycle, with a constant temperature of $22\text{ }^{\circ}\text{C} \pm 2\text{ }^{\circ}\text{C}$ and humidity of $55\% \pm 5\%$. Food and water were available to the mice, *ad libitum*. Animals were allowed to acclimate for 7 days after arrival at the Association for Assessment and Accreditation of Laboratory Animal Care (AAALAC)-accredited Yonsei University College of Medicine Animal Care Facilities. All experimental procedures were approved by the Institutional Animal Care and Use Committee of Yonsei University Health System (permit no.: 2022-0114, approval date: 14 June 2022) and adhered to the National Institutes of Health Guidelines.

2. Experimental designs

Based on several research studies that have developed animal models of CIPN using cisplatin, an experiment was designed to induce peripheral neuropathy by administering cisplatin to a minimum. As this study aimed to carry out experiments once peripheral neuropathy was established, a series of assessments including up-down tests and acetone tests were performed on day 7 and day 14 to validate the maintenance of peripheral neuropathy following two cisplatin administrations. The open field tests were performed on day 8 and day 15 to assess the locomotor activity following two cisplatin administrations. The experimental results from day 7 (day 8) and day 14 (day 15) were compared with previously findings,⁵⁰ and based on this, further studies were conducted on day 14. The experiments in this study were divided into two parts. In experiment 1, the study objected to validate the pain-relieving effects of JZL195 in the CIPN animal model and to

characterize the effects of JZL195 specifically through cannabinoid receptors and TLR4 in glial cells. In Experiment 2, the study sought to further refine the behavioral effects of JZL195 by identifying the specific areas within the CIPN animal model responsible for the pain-relieving effects of JZL195 observed in experiment 1.

Experiment 1 was designed to determine whether JZL195 can relieve pain in the CIPN model. Both up-down tests and acetone tests were carried out on day 14. The concentrations of JZL195 used in this study were categorized as low (3 mg/kg), medium (10 mg/kg), and high (20 mg/kg), based on previous reports.^{51,52} Consequently, tests were conducted in five groups. This experiment established the optimal concentration and time point of JZL195 that demonstrated the most effective pain-relieving effect. Additionally, the movement of the mice was recorded through the open field test and subsequently analyzed to assess the effect of JZL195 on locomotor activity. After administering JZL195 to the CIPN animal model, western blots were performed to identify changes in glial cells and ECS in the DRG and spinal cord, as well as to further investigate changes in TLR4 and inflammatory factors. In addition, immunohistochemistry staining was performed to determine whether glial cells, cannabinoid receptors, and TLR4 were altered after JZL195 administration, and to identify potential correlations between ECS and TLR4.

Experiment 2 was designed to determine the specific location where JZL195 acts to relieve pain. To achieve this, either AM251, a CB1R antagonist, or AM630, a CB2R antagonist, was directly administered into the intrathecal cavity 1.5 h after the JZL195 administration on day 14. Both the up-down test and acetone test were performed, and the subjects were divided into five groups. . The concentrations of AM251 and AM630 used in the experiments were set as low (0.01 mg/kg) and high (0.03 mg/kg), based on previous studies.^{53,54}

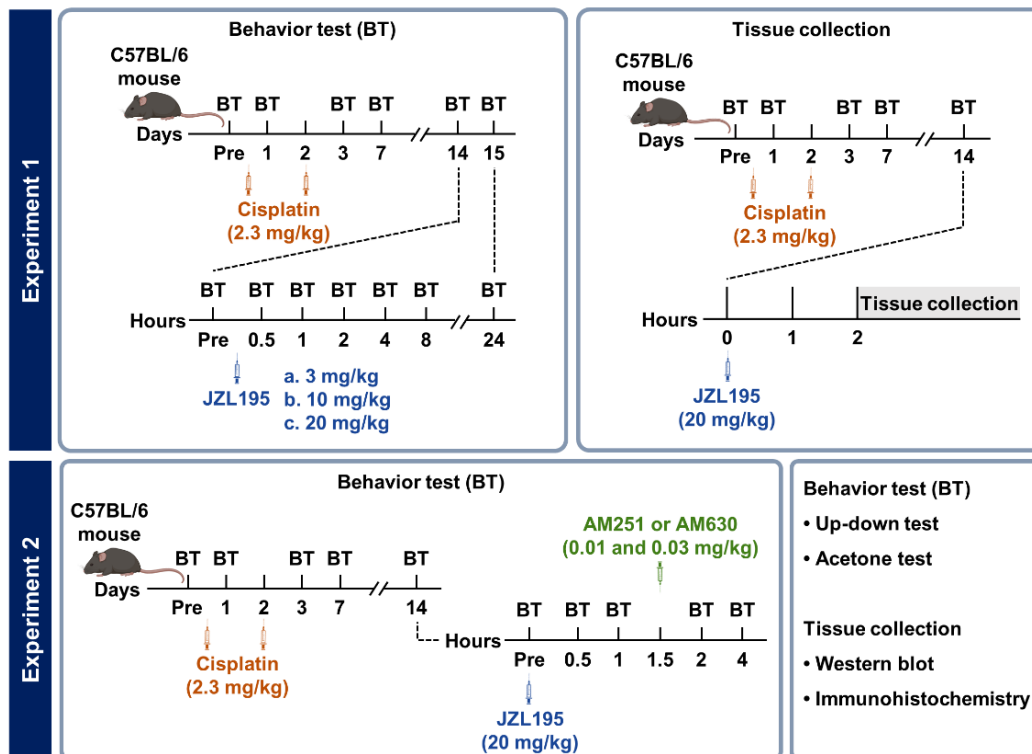


Figure 1. An illustration of overall experimental design. The illustration delineates the days of drug administration and the behavioral tests performed in this study.

3. Drugs

Cisplatin (cis-Diammineplatinum(II) dichloride) was obtained from Sigma-Aldrich (P4394; St. Louis, MO, USA). JZL195 (4-[(3-Phenoxyphenyl)methyl]-1-piperazinecarboxylic acid 4-nitrophenyl ester) was obtained from Tocris Bioscience (4715; Ellisville, MO, USA). AM251 (1-(2,4-dichlorophenyl)-5-[4-iodophenyl]-4-methyl-N-1-piperidinyl-1H-pyrazole-3-carboxamide) and AM630 ([6-iodo-2-methyl-1-[2-(4-morpholinyl)ethyl]-1H-indol-3-yl][4-methoxyphenyl]methanone-6-iodopravodoline) were

obtained from Cayman Chemical (71670; 10006974; Ann Arbor, MI, USA). All drugs were prepared just before administration. Cisplatin was diluted in sterile normal saline (0.9% NaCl). JZL195, AM251, and AM630 were dissolved in DMSO and diluted in ethanol, cremophor, and sterile normal saline at a final ratio of 1:1:18.

4. Chemotherapy-induced peripheral neuropathy model

To induce a CIPN model, C57BL/6 mice were injected with cisplatin (2.3 mg/kg; i.p.) twice every other day, following the concentration and frequency used in previous CIPN studies.^{34,55,56} Control groups for cisplatin-induced peripheral neuropathy received sterile normal saline instead of cisplatin. Previous studies have shown that cisplatin is known to cause weight loss after administration. Therefore, the mice were weighed before cisplatin administration (Pre), and after the first cisplatin administration (day 1) and the second cisplatin administration (day 3). Mice that lost 20% of their body weight after cisplatin administration were excluded from the study. However, in this study, none of the mice lost more than 20% of their body weight, and accordingly all mice were included. Additionally, the mice were weighed on day 7 and day 14.

5. JZL195, AM251 and AM630 injections

JZL195, AM251, and AM630 were used in this study. JZL195 was administered on day 14 after the completion of the Pre behavioral test. JZL195 at concentrations of 3, 10, and 20 mg/kg were administered intraperitoneally (i.p.) to mice in the cisplatin group. AM251 and AM630 were used as antagonists of JZL195 and were administered 1.5 h after JZL195 administration. The injection time of AM251 and AM630 was set to be 30 min earlier than the time when JZL195 exhibited its maximum effectiveness. Both antagonists were administered intrathecally (i.t.) at 0.01 mg/kg and 0.03 mg/kg. Mice were anesthetized with isoflurane (Hana Pharm, Seongnam, Gyeonggi, South Korea), and the hair on their back

was gently shaved to facilitate the identification of the lumbar 5 level. The antagonists were then slowly injected into the spinal cavity using a 31-gauge needle. Following the administration of antagonists, needle was withdrawn after 5 min to prevent the chemicals from refluxing.

6. Behavioral tests

A. Mechanical allodynia assessment

To estimate the response to the mechanical stimulus, an up-down test was conducted. The 50% withdrawal thresholds in response to a series of eight von Frey hairs (2.44 to 4.31 g) were examined using the up-down method, as described previously, starting with a 3.61 g filament (Stoelting, Wood Dale, IL, USA).^{57,58} Clear acrylic cages were placed on mesh platforms, and the mice were placed inside the cages. The mice were habituated for 30 min to 1 h before the 50% withdrawal thresholds were measured by applying filaments to the paw pad of the mice. The filament was held for 3–5 sec to fully deliver the mechanical stimulus. Withdrawal, licking, and flinching of the hind paw were considered as responses to the von Frey filament.

B. Cold allodynia assessment

To evaluate the response to a cold stimulus, an acetone test was conducted. After the up-down test, mice were habituated for an additional 30 min on mesh platforms with clear acrylic cages to assess cold allodynia. Acetone was prepared in a 1-ml syringe with a blunt tip to avoid any mechanical stimulation. Acetone was dispensed at the end of the blunt tip and applied to the paw pad. To assess both immediate and delayed responses to acetone, the behavior of the mice was monitored for 5 min following acetone application. Withdrawal, licking, and flinching were considered as responses, and five responses were

collected and recorded as data.

C. Open field test (OFT)

One day before OFT recording, the mouse cages were placed in the room where the OFT was to be conducted, allowing the mice to become accustomed to the space. On testing day, mice were placed in the transparent apparatus (43 cm length × 43 cm width × 30 cm height) and were given 30 min to habituate. Locomotor activities were measured for 10 min after habituation and when the recording was completed, the transparent apparatus was wiped with 10% ethanol for next behavioral session. Locomotor activities were recorded and analyzed using a photosensor system (Super Flex; Fusion software; Omnitech Electronics Inc., Columbus, OH, USA). All OFTs, including habituation and recording, were conducted between 8:00 am and 6:00 pm.

7. Western blot analysis

Western blot analysis was performed to evaluate the expression levels of FAAH, MAGL, CB1R, CB2R, TLR4, TNF- α , IL-1 β , GFAP, and ionized calcium binding adaptor molecule 1 (Iba1) in the DRG and spinal cord. Mice were anesthetized with isoflurane (Hana Pharm) and euthanized for tissue collection on day 14. The L1-L6 level of the DRG and the L4-L6 level of the spinal cord were collected immediately and stored at -70°C for further tests. The tissues were homogenized with a mixture of lysis buffer (PRO-PREP; Intron Biotechnology, Pyeongtaek, Korea) and a protease inhibitor cocktail (P8340; Sigma-Aldrich). The samples were then sonicated and centrifuged at 15,000 rpm for 10 min, and the supernatants containing proteins were decanted into a clean tube. The protein concentration was measured using a BCA kit. For western blot analysis, samples with 20 μg of total protein were prepared and loaded into an 8–12% acrylamide gel, and then transferred onto a PVDF transfer membrane (Merck Millipore, Darmstadt, Germany). The

PVDF membranes were incubated in 5% skim milk (SM2010; Georgiachem, Norcross, GA, USA) for 1 h at room temperature (RT), and then incubated with the primary antibody overnight at 4 °C. FAAH (101600; Cayman Chemical; 1:500), MAGL (100035; Cayman Chemical; 1:500), CB1R (PA5-85080; Invitrogen, Waltham, MA, USA; 1:10000), CB2R (#703485; Invitrogen; 1:5000), TLR4 (PA5-23125; Invitrogen; 1:1000), TNF- α (ab66579; Abcam, Cambridge, UK; 1:1000), IL-1 β (ab9722; Abcam; 1:10000), GFAP (ab279291; Abcam; 1:1000), Iba1 (ab283346; Abcam; 1:1000), and GAPDH (LF-PA0018; AbFrontier; 1:10000) in 5% bovine serum albumin (Sigma-Aldrich) with 1x TBST were used as primary antibodies. The membrane was then incubated with secondary anti-rabbit antibody (#7074; CTS; 1:5000) and anti-mouse antibody (#7076; CTS; 1:5000) for 2 h at room temperature. Enhanced chemiluminescence select detection reagent (ECL; Cytiva) was used to visualize the antibody-labeled protein bands. The bands were detected using Cytiva (IQ800), and the intensities were quantified using ImageJ.

8. Immunohistochemistry staining

The animals were anesthetized with pentobarbital (50 mg/kg, i.p.) and then perfused transcardially with 0.9% sterile normal saline, followed by 4% paraformaldehyde in phosphate buffer saline (PBS) (pH 7.4). The DRG and spinal cord were extracted and post-fixed overnight at 4 °C before cryoprotecting in 30% sucrose in 1x PBS for 24 h. The tissues were placed in a mold and covered with Optimal Cutting Temperature (O.C.T.; Sakura Finetek, Torrance, CA, USA). Subsequently they were rapidly frozen using liquid nitrogen and stored at -70 °C for further testing. The tissues were sectioned transversely (14 μ m) using a cryostat (Microm HM525; Thermo Scientific, Waltham, MA, USA). Prior to testing, the slide glasses with the sectioned tissues were incubated in 10 mM sodium citrate buffer to expose antigen sites. The sectioned tissues were washed with 1x PBS for 15 min and then washed with 0.3% PBST (Triton X-100 in 1x PBS) for 15 min. The sectioned tissues were incubated with blocking solution (normal donkey serum in 0.3% PBST) for 1 h, and

then incubated overnight in primary antibodies (primary antibodies in blocking solution) at 4 °C. The primary antibodies used were TLR4 (PA5-23125; Invitrogen; 1:500), CB1R (ab23703; Abcam; 1:500), CB2R (#703485; Invitrogen; 1:1000), GFAP (ab279291; Abcam; 1:500), and Iba1 (ab283346; Abcam; 1:500). The sectioned tissues were washed with 0.3% PBST and incubated for 2 h with secondary antibodies. After an additional wash with 0.3% PBST, DAPI staining (Vectashield mounting medium; Burlingame, CA, USA) was conducted before covering with a cover glass. Images were obtained using a laser scanning confocal microscope (Zeiss LSM 700; Carl Zeiss, Jena, Germany) at 20x magnification for the DRG and 40x magnification for the spinal cord. Representative images were subjected to maximum intensity projection (MIP) and exported using Zen Black software (Carl Zeiss). Quantification of the stained area and mean fluorescence intensity (MFI) with MIP images were processed using Zen Blue software (Carl Zeiss).

9. Statistical analysis

Statistical analyses were performed using GraphPad Prism 10.1.0 (GraphPad Software, San Diego, CA, USA). The behavioral test data for the up-down and acetone tests were analyzed using a two-way analysis of variance (ANOVA) with repeated measures, followed by Bonferroni's test for post hoc comparisons. The behavioral test data for the OFT between two groups were analyzed using t-tests and Mann-Whitney's non-parametric tests. The OFT data comparing three groups were analyzed using one-way ANOVA and Kruskal-Wallis's non-parametric tests with Dunn's multiple comparison. Western blotting data and IHC data were analyzed by one-way ANOVA followed by Tukey's test for multiple comparisons. The data obtained using the up-down test, acetone test, and western blot are presented as means \pm standard error of the mean (SEM). Data for OFT are expressed as median with interquartile range (IQR). P values less than 0.05 were considered to indicate statistically significant differences.

III. RESULTS

1. Differences in locomotor behaviors on day 8 and day 15 in the CIPN animal model

First, the mechanical and cold allodynia were assessed through the up-down test and acetone test to confirm the development of pain from Pre to day 7 or day 14 (Figure 2A). Next, the OFT was performed on day 8 or day 15 to analyze the movement of mice and to monitor their locomotor activities after cisplatin injection (Figure 2A). The 50% withdrawal thresholds were significantly reduced by cisplatin on day 1 and remained so until day 7 (Figure 2B, for days: $F_{3,54} = 9.656$, $p < 0.0001$; for groups: $F_{1,18} = 38.77$, $p < 0.0001$; for days \times groups interaction: $F_{3,54} = 20.21$, $p < 0.0001$, two-way ANOVA followed by Bonferroni's multiple comparison test). Similarly, the responses to acetone were significantly increased by cisplatin on day 1 and remained so until day 7 (Figure 2C, for days: $F_{3,54} = 26.68$, $p < 0.0001$; for groups: $F_{1,18} = 66.43$, $p < 0.0001$; for days \times groups interaction: $F_{3,54} = 14.09$, $p < 0.0001$, two-way ANOVA followed by Bonferroni's multiple comparison test). On day 8, one day after the up-down test and acetone test were conducted, the mice treated with cisplatin traveled significantly longer distances than the mice treated with the vehicle (Figure 2D and 2E, $p = 0.0152$, unpaired t-test). Meanwhile, there was no significant difference in the movement episode count, which reflects the overall number of locomotor activities, between the vehicle and cisplatin groups on day 8 (Figure 2F, $p = 0.5087$, unpaired t-test). However, on day 8, the mice treated with cisplatin spent significantly more time in movement compared to the mice treated with the vehicle (Figure 2G, $p = 0.0411$, unpaired t-test).

Additionally, the mechanical and cold allodynia were measured from Pre to day 14. The 50% withdrawal thresholds were significantly decreased by cisplatin from day 1 to day 14 (Figure 2H, for days: $F_{4,72} = 17.69$, $p < 0.0001$; for groups: $F_{1,18} = 163.6$, $p < 0.0001$; for days \times groups interaction: $F_{4,72} = 18.93$, $p < 0.0001$, two-way ANOVA followed by Bonferroni's multiple comparison test). Similarly, the responses to acetone were

significantly increased from day 1 to day 14 due to cisplatin (Figure 2I, for days: $F_{4, 72} = 19.00$, $p < 0.0001$; for groups: $F_{1, 18} = 81.52$, $p < 0.0001$; for days \times groups interaction: $F_{4, 72} = 8.468$, $p < 0.0001$, two-way ANOVA followed by Bonferroni's multiple comparison test). These findings demonstrate that a final concentration of 4.6 mg/kg of cisplatin effectively prolongs both mechanical and cold allodynia not only until day 7 but also until day 14. On day 15, the total distance traveled did not show a significant difference between the vehicle and cisplatin groups (Figure 2J and 2K, $p = 0.6991$, unpaired t-test). There was no significant difference in the count of movement episodes between the vehicle and cisplatin groups on day 15 (Figure 2L, $p = 0.2576$, unpaired t-test). Furthermore, there was no significant difference in movement time observed between the vehicle group and cisplatin groups on day 15 (Figure 2M, $p = 0.6991$, unpaired t-test). Previous studies have reported that animals receiving chemotherapy typically display reduced activity due to toxicity or motor neuropathy.⁵⁰ The measurements on day 8 slightly differed from the previously reported results in CIPN animal models, while the OFT results for day 15 were more similar to those reported in the previous CIPN study.⁵⁰

In summary, mechanical and cold allodynia persisted until day 7 and day 14 after administering 4.6 mg/kg of cisplatin twice. Furthermore, on day 15, locomotor activities were similar to those observed in a previous CIPN animal study. Consequently, further tests were conducted on day 14 instead of day 7.

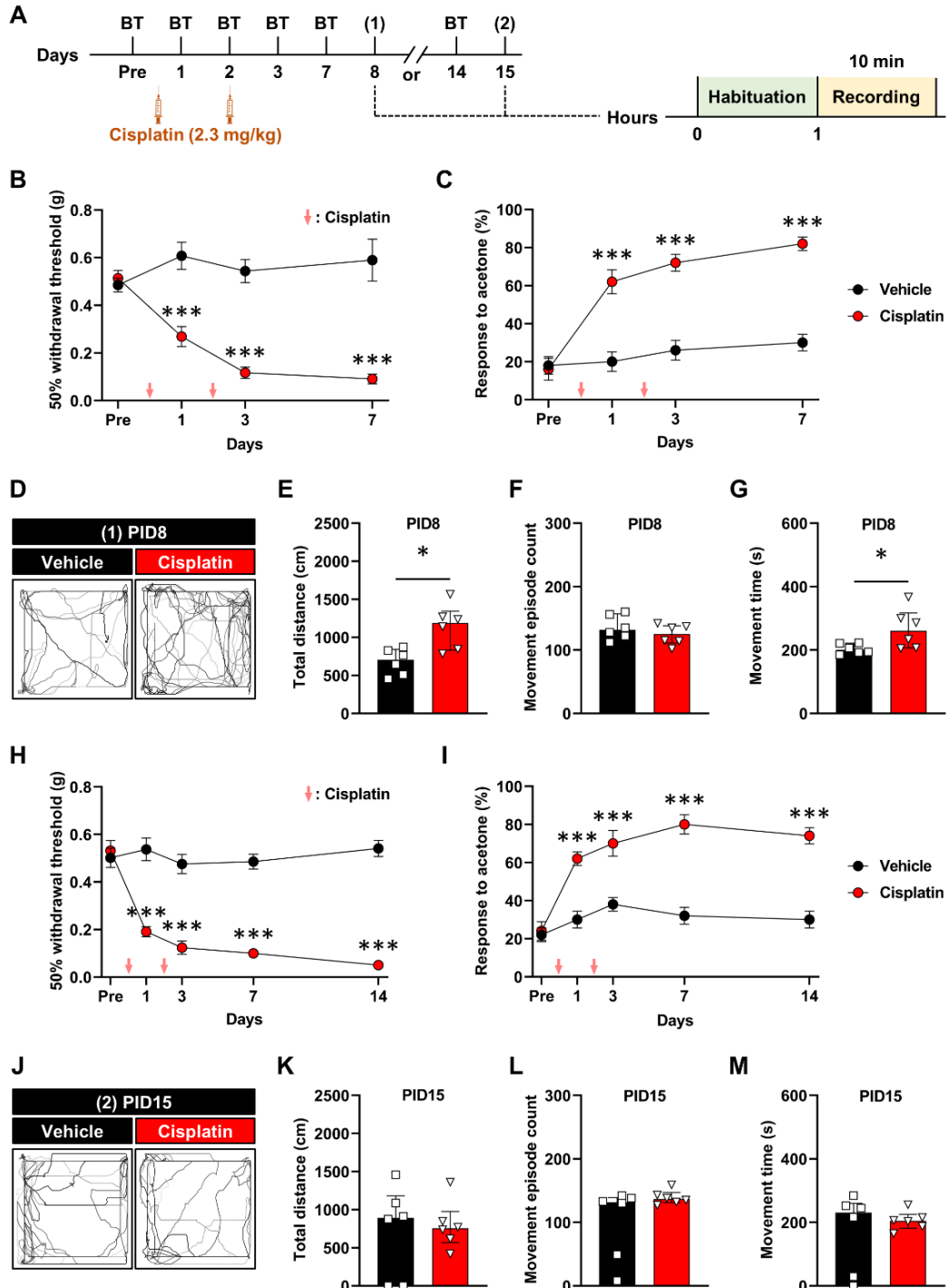


Figure 2. Assessment of the mechanical allodynia, cold allodynia, and locomotor activity of the mice after cisplatin injection. (A) An illustration of experimental timeline for OFT. (B) Development of the mechanical allodynia after cisplatin injection. Cisplatin group showed significant decrease in the 50% withdrawal thresholds from day 1 to day 7 compared to vehicle group (n = 10). Red arrows indicate the 2.3 mg/kg cisplatin injections. (C) Development of the cold allodynia after cisplatin injection. Cisplatin group showed significant increase in the responses to acetone from day 1 to day 7 compared to vehicle group (n = 10). (D) A graphical representation of the distance traveled by mice. The darkening color of the line reflects the passage of time as the mice moves. (E) Measurement of the total distance of the mice on day 8 after cisplatin injection. On day 8, the cisplatin group traveled significantly longer compared to the vehicle group. (F) Measurement of the movement episode count of the mice on day 8 after cisplatin injection. The movement episode count did not exhibit any significant alterations between the vehicle groups and cisplatin groups on day 8. (G) Movement time of the mice on day 8 after cisplatin injection. On day 8, the cisplatin group significantly spent more time to travel when contrasted with the vehicle group. (H) Development of the mechanical allodynia after cisplatin injection. Decreased 50% withdrawal thresholds due to cisplatin administration and the mechanical allodynia was maintained until day 14 (n = 10). (I) Development of the cold allodynia after cisplatin injection. Increased responses to acetone due to cisplatin administration and cold allodynia was maintained until day 14 (n = 10). (J) A graphical representation of the distance traveled by mice. (K) Measurement of the total distance of the mice on day 15 after cisplatin injection. On day 15, there was no significant difference between the two groups. (L) Measurement of the movement episode count of the mice on day 15 after cisplatin injection. The movement episode count did not exhibit any significant

alterations between the vehicle groups and cisplatin groups on day 15. (M) Movement time of the mice on day 15 after cisplatin injection. On day 15, there was no difference in the movement time between the vehicle groups and cisplatin groups. Data for up-down test and acetone test are presented as mean \pm SEM and analyzed by two-way ANOVA followed by Bonferroni's post hoc multiple comparison test. Data for OFT are presented as median with IQR and analyzed by t-test and Mann-Whitney non-parametric test. The significances are marked as * $p < 0.05$ and *** $p < 0.001$, compared with the vehicle group.

2. JZL195 alleviates mechanical and cold allodynia in an animal model of CIPN

Mice were weighed throughout the entire experiment to determine any of them lost more than 20% of their body weight due to cisplatin treatment. Both on day 1 and day 3, the day after cisplatin administration, the body weight of mice in the cisplatin group slightly decreased, but this decrease was not statistically significant compared to the vehicle group. Additionally, none of the mice in the cisplatin group lost over 20% of their body weight (Figure 3A, for days: $F_{5, 650} = 226.2$, $p < 0.0001$; for groups: $F_{4, 130} = 1.840$, $p = 0.1251$; for days \times groups interaction: $F_{20, 650} = 1.268$, $p = 0.1932$, two-way ANOVA).

To substantiate the analgesic effect of JZL195, all tests were conducted on day 14. In line with previous results, mice treated with cisplatin showed a significant decrease in the 50% withdrawal thresholds, indicating the establishment and maintenance of mechanical allodynia until day 14 (Figure 3B, for days: $F_{4, 240} = 256.1$, $p < 0.0001$; for groups: $F_{4, 60} = 152.0$, $p < 0.0001$; for days \times groups interaction: $F_{16, 240} = 14.93$, $p < 0.0001$, two-way ANOVA followed by Bonferroni's multiple comparison test). On day 14, the mice underwent a Pre behavioral test, which was the final test for the development of CIPN (day 14) and served as a baseline test for JZL195 administration (Pre). Subsequently, three different concentrations (3, 10, and 20 mg/kg) of JZL195 were administered to determine the most effective concentration with analgesic properties. The analgesic effects of

JZL195 on mechanical and cold allodynia were assessed through the up-down test and acetone test at 0.5, 1, 2, 4, 8, and 24 h following JZL195 administration. In the up-down test, mice receiving 3 mg/kg of JZL195 (Cis + 3 mg/kg JZL195) did not show any significant changes in the 50% withdrawal thresholds compared to mice receiving the vehicle (Cis + Veh). In contrast, mice receiving 10 mg/kg of JZL195 (Cis + 10 mg/kg JZL195) demonstrated a significant increase in the 50% withdrawal thresholds compared to mice receiving the vehicle (Cis + Veh) at 2 h after JZL195 administration. This indicates that administering 10 mg/kg of JZL195 provides pain relief at 2 h, but the effect does not last beyond this point. Mice receiving 20 mg/kg of JZL195 (Cis + 20 mg/kg JZL195) displayed a significant analgesic effect in mechanical allodynia at 1 and 2 h, with the most pronounced effect observed at 2 h, compared to mice receiving the vehicle (Cis + Veh) (Figure 3C, for time: $F_{6, 360} = 16.57$, $p < 0.0001$; for groups: $F_{4, 60} = 351.4$, $p < 0.0001$; for time \times groups interaction: $F_{24, 360} = 5.356$, $p < 0.0001$, two-way ANOVA followed by Bonferroni's multiple comparison test). In the acetone test, cisplatin significantly increased responses to acetone, indicating the development and persistence of cold allodynia until day 14 (Figure 3D, for days: $F_{4, 260} = 79.40$, $p < 0.0001$; for groups: $F_{4, 65} = 44.82$, $p < 0.0001$; for days \times groups interaction: $F_{16, 260} = 3.572$, $p < 0.0001$, two-way ANOVA followed by Bonferroni's multiple comparison test). In the acetone test, 3 and 10 mg/kg of JZL195 (Cis + 3 mg/kg JZL195 and Cis + 10 mg/kg JZL195) did not produce a significant analgesic effect compared to mice receiving the vehicle (Cis + Veh). However, a significant increase in responses to acetone was observed 2 h after the administration of 20 mg/kg JZL195 (Cis + 20 mg/kg JZL195) compared to mice receiving the vehicle (Cis + Veh) (Figure 3E, for time: $F_{6, 390} = 13.31$, $p < 0.0001$; for group: $F_{4, 65} = 50.54$, $p < 0.0001$; for time \times group interaction: $F_{24, 390} = 1.904$, $p = 0.0068$, two-way ANOVA followed by Bonferroni's multiple comparison test).

Taken together, these results suggest that the optimal concentration of JZL195 to alleviate mechanical and cold allodynia is 20 mg/kg. Moreover, the analgesic effect of JZL195 peaks at 2 h after administration.

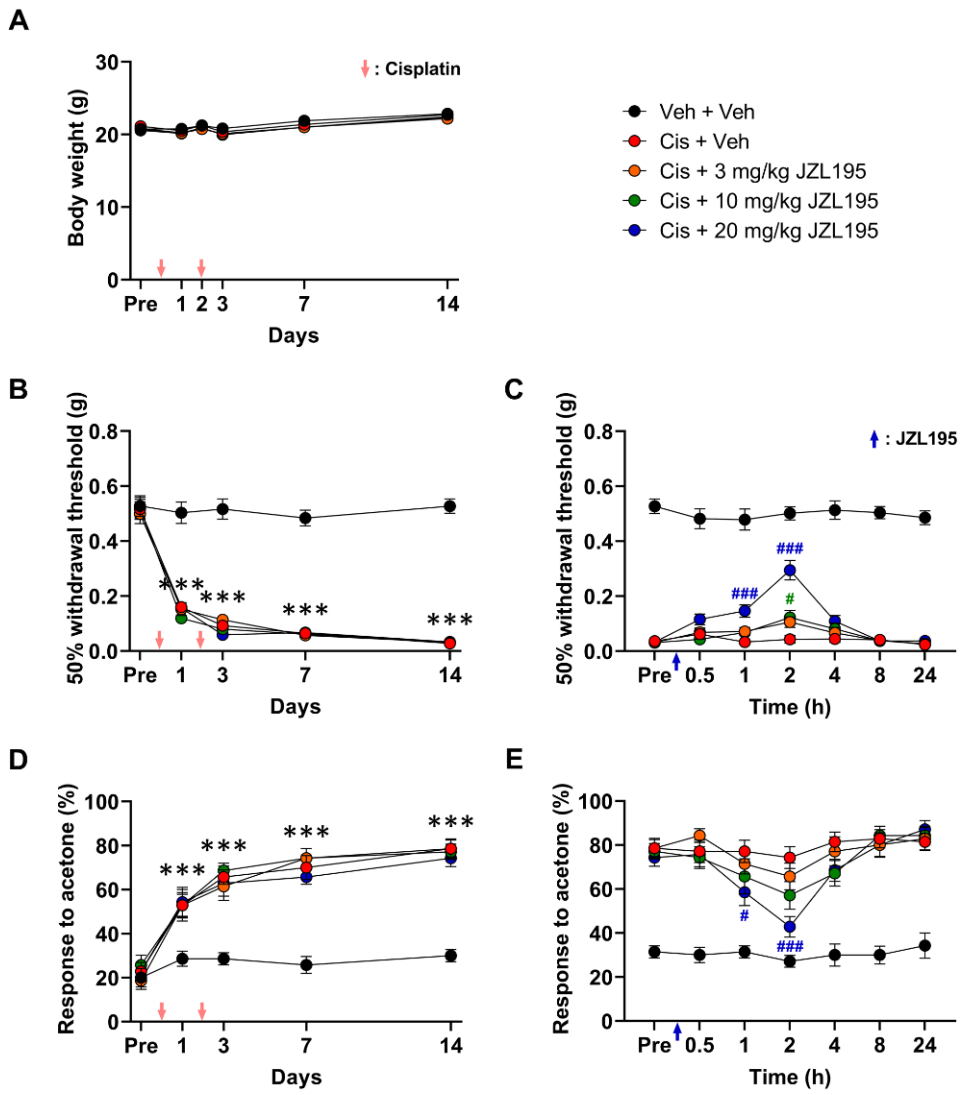


Figure 3. Assessment of the mechanical allodynia, cold allodynia, and body weight in CIPN animal model after JZL195 administration. (A) The body weights were measured through overall experimental. The body weight of the cisplatin groups (Cis + Veh, Cis + 3 mg/kg JZL195, Cis + 10 mg/kg JZL195, and Cis + 20 mg/kg JZL195) tended to decrease on day 1 and day 3. However, the decrease in the body weight was not greater

than 20% and was not statistically significant when compared to the vehicle group (Veh + Veh) (n = 27). A red arrows indicate the 2.3 mg/kg cisplatin injections. (B) Development of the mechanical allodynia after cisplatin injection. The cisplatin groups (Cis + Veh, Cis + 3 mg/kg JZL195, Cis + 10 mg/kg JZL195, Cis + 20 mg/kg JZL195) showed significant decrease in the 50% withdrawal thresholds from day 1 to day 14 (n = 13). (C) The pain-relieving effect of JZL195 on the mechanical allodynia. 10 mg/kg of JZL195 significantly attenuated 50% withdrawal thresholds after 2 h, while 20 mg/kg of JZL195 significantly attenuated 50% withdrawal thresholds after 1 and 2 h (n = 13). A blue arrow indicates the JZL195 administrations. (D) Development of the cold allodynia after cisplatin injection. The cisplatin groups (Cis + Veh, Cis + 3 mg/kg JZL195, Cis + 10 mg/kg JZL195, Cis + 20 mg/kg JZL195) showed significant increase in the responses to acetone from day 1 to day 14 (n = 14). (E) The pain-relieving effect of JZL195 on the cold allodynia. 20 mg/kg of JZL195 significantly alleviated responses to acetone after 1 and 2 h (n = 14). Data are presented as mean \pm SEM and analyzed by two-way ANOVA followed by Bonferroni's post hoc multiple comparison test. The significances are marked as ***p < 0.001, compared with the Veh + Veh group. The significances are marked as #p < 0.05 and ###p < 0.001, compared with the Cis + Veh group.

3. JZL195 with locomotor activity in the CIPN animal model

To analyze the impact of JZL195 on locomotor activities in the CIPN animal model, the movements of the mice were measured using the OFT 2 h after JZL195 administration (Figure 4A). The total distance traveled by the mice treated with vehicle (Veh + Veh) was slightly greater compared to the mice treated with cisplatin (Cis + Veh). The total distance traveled by the mice treated with JZL195 (Cis + JZL) was reduced compared to the mice treated with vehicle (Veh + Veh). However, these results were not statistically significant (Figure 4B, for Veh + Veh: p = 0.3568; for Cis + JZL: p = 0.6924, one-way ANOVA). The movement episode counts of the mice treated with vehicle (Veh + Veh) were slightly higher

than those of the mice treated with cisplatin (Cis + Veh). The mice treated with JZL195 (Cis + JZL) also showed a slight increase in their movement counts compared to the mice treated with cisplatin (Cis + Veh). However, no statistically significant difference was observed among the three groups (Figure 4C, for Veh + Veh: $p = 0.0887$; for Cis + JZL: $p = 0.2098$, one-way ANOVA). The total movement time of the mice treated with vehicle (Veh + Veh) was higher, while the mice treated with JZL195 (Cis + JZL) had a lower total movement time compared to the mice treated with cisplatin (Cis + Veh). However, these changes were not statistically significant (Figure 4D, for Veh + Veh: $p = 0.1919$; for Cis + JZL195: $p = 0.4197$, one-way ANOVA). There was no significant difference in resting time among the three groups (Figure 4E, for Veh + Veh: $p = 0.2218$; for Cis + JZL195: $p > 0.9999$, one-way ANOVA).

The OFT areas were divided into outer and inner zones, and the total distance traveled and movement time were measured in each zone (Figure 4F, G, H, and I). The total distance traveled in the outer zone was higher in the vehicle group (Veh + Veh) compared to the cisplatin group (Cis + Veh) (Figure 4F, $p = 0.3866$, one-way ANOVA). The total distance traveled by the mice treated with JZL195 (Cis + JZL) was lower compared to the cisplatin groups (Cis + Veh) (Figure 4F, $p = 0.6474$, one-way ANOVA). However, these differences were not statistically significant. Similarly, there were no significant variations in the total distance traveled in the inner zone among the three groups (Figure 4G, for Veh + Veh: $p = 0.0815$; for Cis + JZL195: $p > 0.9999$, one-way ANOVA). There was no significant variations within any of the three groups in the total duration spent in the outer zone (Figure 4H, for Veh + Veh: $p = 0.1919$; for Cis + JZL195: $p = 0.4197$, one-way ANOVA). Furthermore, there was no significant changes in the total duration spent in inner zone (Figure 4I, for Veh + Veh: $p = 0.0815$; for Cis + JZL195: $p > 0.9999$, one-way ANOVA). The vertical episode count and vertical activity time, which measure the number and time of movements corresponding to rearing, did not exhibit significant differences among the three groups (Figure 4J, for Veh + Veh: $p = 0.1364$; for Cis + JZL195: $p > 0.9999$, one-way ANOVA; and 4K, for Veh + Veh: $p = 0.3318$; for Cis + JZL195: $p > 0.9999$, one-way ANOVA).

ANOVA). Also, the number of stereotypic episodes did not display any noticeable difference among the three groups (Figure 4L, for Veh + Veh: $p = 0.1204$; for Cis + JZL195: $p = 0.5385$, one-way ANOVA). However, the duration of stereotypic behavior was significantly reduced in the cisplatin group (Cis + Veh) compared to the vehicle group (Veh + Veh) (Figure 4M, for Veh + Veh: $p = 0.0189$; for Cis + JZL195: $p = 0.4860$, one-way ANOVA followed by Dunn's multiple comparison test). These results suggest that cisplatin has the potential to reduce locomotor activity-associated behaviors and that JZL195 does not substantially impact the locomotor activities in the CIPN animal model.

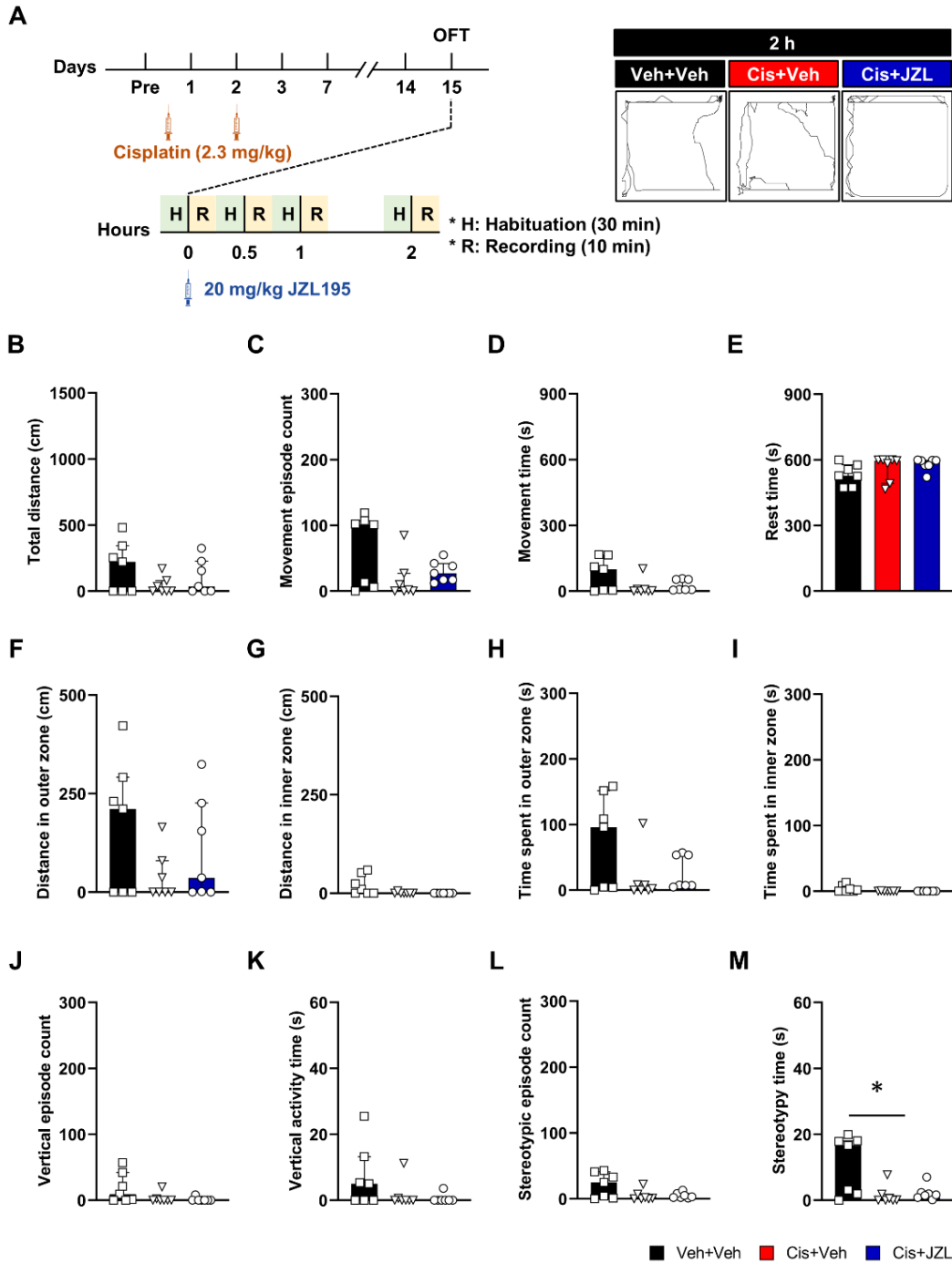


Figure 4. Assessments of locomotor activities of the CIPN mice after JZL195 administration on day 15. (A) An illustration of experimental timeline for OFT and a graphical representation of the distance traveled by mice. (B) Measurement of total distance. There was no significant difference in the total distance traveled by the mice among three groups ($n = 7$). (C) Measurement of movement episode count. The movement episode counts in cisplatin groups (Cis + Veh and Cis + JZL195) were decreased compared to the vehicle group (Veh + Veh), but statistically not significant ($n = 7$). (D) Measurement of movement time. The total movement time showed no significant difference among three groups ($n = 7$). (E) Measurement of rest time. There was no statistically significant difference in the rest time among the three groups, indicating that the mice in three groups rested for a similar duration ($n = 7$). (F) Analysis of distance in outer zone ($n = 7$). (G) Analysis of distance in inner zone ($n = 7$). No significant difference was observed in the total distance traveled within the outer and inner zones between the three groups. (H) The amount of time that the mice traveled in the outer zone ($n = 7$). (I) The amount of time that the mice traveled in the inner zone ($n = 7$). The movement time in the outer and inner zones between the three groups did not exhibit a significant difference. (J) Assessment of vertical episode count ($n = 7$). (K) Assessment of vertical activity time ($n = 7$). There was no significant difference in the number of vertical activity as well as vertical activity time among three groups. (L) Assessment of stereotypy episode count ($n = 7$). (M) Assessment of stereotypy time ($n = 7$). The stereotypy episode count in mice did not show significant difference between the three groups, while the stereotypy time was significantly reduced in the cisplatin group (Cis + Veh) compared to the vehicle group. Data are presented as median with IQR and analyzed by one-way ANOVA followed by Dunn's multiple comparison test or Kruskal-Wallis non-parametric test. The significances are marked as $*p < 0.05$, compared with the Cis + Veh group.

4. JZL195 inhibited FAAH/MAGL and regulated the cannabinoid receptors differently in the DRG and spinal cord

To analyze the changes in expression of FAAH, MAGL, CB1R, and CB2R in the DRG and spinal cord, western blot analyses were performed 2 h after administering JZL195 on day 14. First, the western blot results of the DRG revealed that FAAH expression levels were significantly upregulated in the cisplatin group (Cis + Veh), while FAAH levels in the JZL195 group (Cis + JZL) were decreased (Figure 5A, $F_{2, 15} = 7.299$, $p = 0.0061$, one-way ANOVA followed by Tukey's multiple comparison test). The changes in MAGL expression were consistent with those of FAAH (Figure 5B, $F_{2, 15} = 5.933$, $p = 0.0126$, one-way ANOVA followed by Tukey's multiple comparison test). However, CB1R expression in the cisplatin group (Cis + Veh) showed a significant increase, whereas in the JZL195 group (Cis + JZL), the expression of CB1R, which was significantly upregulated by cisplatin, decreased (Figure 5C, $F_{2, 15} = 7.005$, $p = 0.0071$, one-way ANOVA followed by Tukey's multiple comparison test). The alterations in CB2R expression within the DRG were similar to those in CB1R expression. CB2R expression notably increased in the cisplatin group (Cis + Veh) compared to the vehicle group (Veh + Veh) but decreased in the JZL195 group (Cis + JZL) (Figure 5D, $F_{2, 15} = 5.086$, $p = 0.0206$, one-way ANOVA followed by Tukey's multiple comparison test).

Spinal cord samples, analyzed using western blot, showed similar results to those observed in the DRG. FAAH levels were significantly upregulated in the cisplatin group (Cis + Veh), while they declined in the JZL195 group (Cis + JZL) (Figure 5E, $F_{2, 18} = 5.229$, $p = 0.0162$, one-way ANOVA followed by Tukey's multiple comparison test). Another catabolic enzyme, MAGL, exhibited comparable alterations to FAAH. MAGL expression in the cisplatin group (Cis + Veh) significantly increased, while it notable decreased in the JZL195 group (Cis + JZL) (Figure 5F, $F_{2, 18} = 6.126$, $p = 0.0093$, one-way ANOVA followed by Tukey's multiple comparison test). These results indicate that cisplatin

significantly increases the expression of FAAH and MAGL, but this upregulated expression is inhibited by JZL195. The expression levels of the two primary cannabinoid receptors differed from those of FAAH and MAGL. In addition, the alterations in CB1R expression within the spinal cord differed from those observed in the DRG. In the spinal cord, CB1R expression in the cisplatin group (Cis + Veh) tended to increase, but this effect was not significant, while CB1R expression in the JZL195 group (Cis + JZL) significantly increased compared to the vehicle group (Veh + Veh) (Figure 5G, $F_{2, 15} = 3.993$, $p = 0.0407$, one-way ANOVA followed by Tukey's multiple comparison test). CB2R expression changes were similar to those of CB1R (Figure 5H, $F_{2, 15} = 3.997$, $p = 0.0406$, one-way ANOVA followed by Tukey's multiple comparison test). These findings indicate that JZL195 differentially regulates catabolic enzymes and cannabinoid receptors in the spinal cord. In summary, findings suggest that JZL195 regulates the ECS differently depending on its location within the pain processing region.

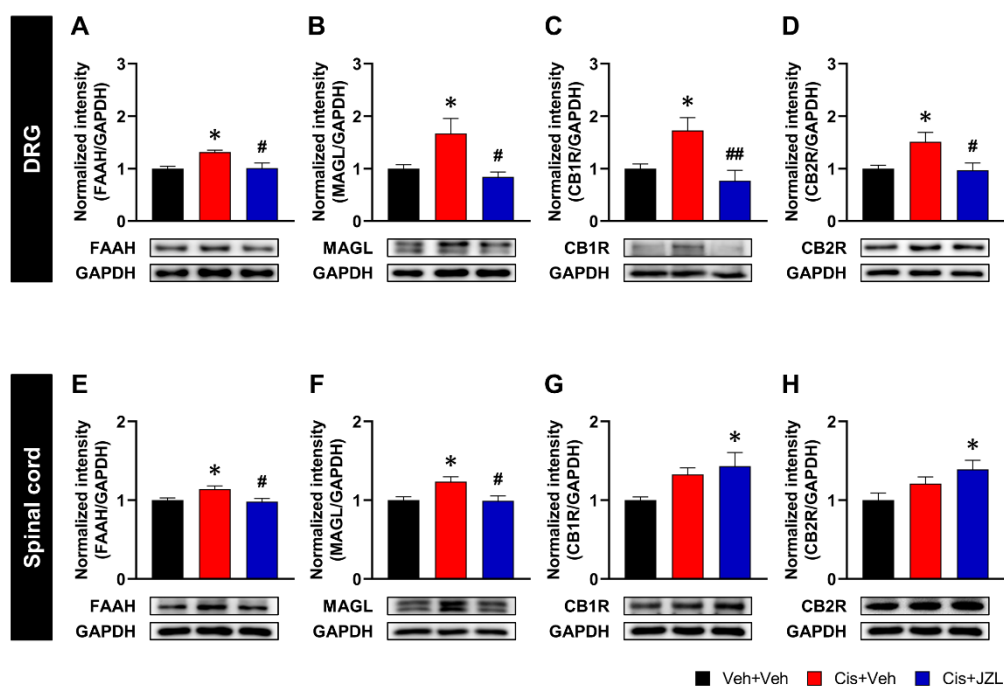


Figure 5. The representative western blot images and quantification of FAAH, MAGL, CB1R, and CB2R expression level in the L4-L6 DRG and spinal cord. (A) The expression of FAAH in Cis + Veh group significantly upregulated compared to Veh + Veh group. However, administration of the JZL195 notably inhibited the expression of FAAH in Cis + JZL group (n = 6). (B) The expression of MAGL in Cis + Veh group was significantly increased compared to Veh + Veh group, whereas administration of the JZL195 notably inhibited the expression of MAGL in Cis + JZL group (n = 6). (C) The expression of CB1R was significantly increased in Cis + Veh groups. Increased expression of CB1R was notably decreased by JZL195 administration (n = 6). (D) Like CB1R, CB2R also showed significant upregulation in the expression compared to Veh + Veh group (n = 6). (E) The expression of FAAH in the Cis + Veh group was significantly increased compared to the Veh + Veh group, whereas administration of the JZL195 notably inhibited the expression of FAAH in Cis + JZL group (n = 7). (F) The Cis + Veh group showed a significant increase in expression of MAGL compared to Veh + Veh group. However, administration of the JZL195 notably inhibited the expression of MAGL in Cis + JZL group (n = 7). (G) The expression of CB1R was significantly increased in Cis + JZL group compared to Veh + Veh group (n = 7). (H) There was similar change in expression of CB2R to CB1R in the spinal cord (n = 7). Data are presented as mean \pm SEM and analyzed by one-way ANOVA followed by Tukey's multiple comparison test. The significances are marked as * $p < 0.05$, compared with the Veh + Veh group. The significances are marked as # $p < 0.05$ and ## $p < 0.01$, compared with the Cis + Veh group.

5. FAAH/MAGL inhibition decreased the TLR4 and pro-inflammatory factors in the DRG and spinal cord

A western blot analysis was performed to measure changes in the expression of TLR4 and pro-inflammatory factors in the DRG and spinal cord. First, TLR4 and pro-inflammatory factors were examined in the DRG. The expression of TLR4 was significantly increased in the cisplatin group (Cis + Veh) compared to the vehicle group (Veh + Veh), and then significantly decreased in the JZL195 group (Cis + JZL) (Figure 6A, $F_{2, 15} = 8.961$, $p = 0.0028$, one-way ANOVA followed by Tukey's multiple comparison test). The level of tumor necrosis factor alpha (TNF- α), a known pro-inflammatory factor, was substantially upregulated by cisplatin (Cis + Veh) in the DRG compared to the control group (Veh + Veh). In contrast, the group that received JZL195 (Cis + JZL) showed a significant reduction in TNF- α expression in the DRG (Figure 6B, $F_{2, 15} = 9.317$, $p = 0.0023$, one-way ANOVA followed by Tukey's multiple comparison test). The expression of Interleukin 1 beta (IL-1 β), another well-known inflammatory factor like TNF- α , noticeably increased in the DRG of the cisplatin group (Cis + Veh) compared to the vehicle group (Veh + Veh). However, following the administration of JZL195 (Cis + JZL), the expression of IL-1 β was significantly reduced compared to the cisplatin group (Cis + Veh) (Figure 6C, $F_{2, 15} = 4.761$, $p = 0.0251$, one-way ANOVA followed by Tukey's multiple comparison test).

When comparing TLR4 expression in the cisplatin group (Cis + Veh) to that in the vehicle group (Veh + Veh), it was found that the expression of TLR4 in the spinal cord was significantly increased by cisplatin. The levels of TLR4 expression, which were upregulated by cisplatin, showed a significant reduction following JZL195 treatment (Cis + JZL) (Figure 6D, $F_{2, 18} = 5.085$, $p = 0.0178$, one-way ANOVA followed by Tukey's multiple comparison test). The level of TNF- α was also significantly upregulated upon cisplatin treatment (Cis + Veh) in the spinal cord compared to the control group (Veh + Veh). However, the group that received JZL195 (Cis + JZL) showed a significant reduction in TNF- α expression in the spinal cord (Figure 6E, $F_{2, 15} = 5.972$, $p = 0.0124$, one-way

ANOVA followed by Tukey's multiple comparison test). Furthermore, the expression of IL-1 β noticeably increased in the spinal cord of the cisplatin group (Cis + Veh) compared to the vehicle group (Veh + Veh). However, following the administration of JZL195 (Cis + JZL), the expression of IL-1 β was significantly reduced compared to the cisplatin group (Cis + Veh) (Figure 6F, $F_{2, 15} = 6.602$, $p = 0.0088$, one-way ANOVA followed by Tukey's multiple comparison test). These results suggest that JZL195 has the potential to alleviate neuroinflammation in CIPN animal models by inhibiting FAAH and MAGL, as it effectively reduced the levels of TLR4 and inflammatory factors that were upregulated by cisplatin.

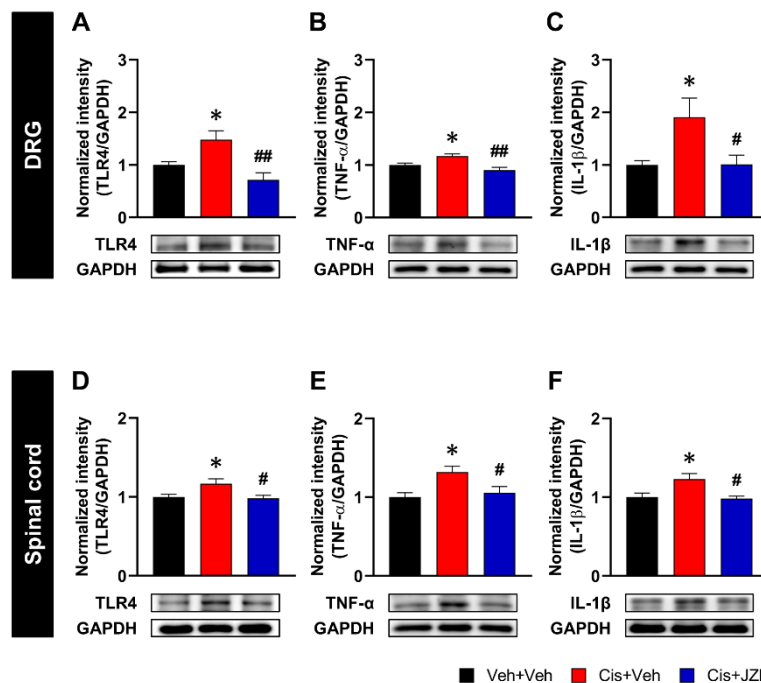


Figure 6. The representative western blot images and quantification of TLR4, TNF- α , and IL-1 β expression level in the L4-L6 DRG and spinal cord. (A) The expression of TLR4 in Cis + Veh group was significantly upregulated compared to Veh + Veh group, while the expression of TLR4 in Cis + JZL group was significantly decreased compared to Cis + Veh group (n = 6). (B) The

expression of TNF- α in Cis + Veh group was significantly increased compared to Veh + Veh group, meanwhile the expression of TNF- α in Cis + JZL group was notably decreased following JZL195 administration (n = 6). (C) In the Cis + Veh group, the expression of IL-1 β was significantly increased compared to Veh + Veh group, whereas the expression of IL-1 β in Cis + JZL195 group was notably decreased after JZL195 administration (n = 6). (D) The expression of TLR4 in Cis + Veh group was significantly increased compared to Veh + Veh group, while the expression of TLR4 in Cis + JZL group was significantly decreased compared to Cis + Veh group (n = 7). (E) In the Cis + Veh group, the expression of TNF- α was significantly increased compared to Veh + Veh group, whereas the expression of TNF- α in Cis + JZL group was notably decreased after JZL195 administration (n = 6). (F) In the Cis + Veh group, the expression of IL-1 β , a pro-inflammatory factor, was significantly increased compared to Veh + Veh group, meanwhile the Cis + JZL group showed decreased expression of IL-1 β after JZL195 administration (n = 6). Data are presented as mean \pm SEM and analyzed by one-way ANOVA followed by Tukey's multiple comparison test. The significances are marked as *p < 0.05, compared with the Veh + Veh group. The significances are marked as #p < 0.05 and ##p < 0.01, compared with the Cis + Veh group.

6. The regulation of glial cell activation in the DRG and spinal cord after FAAH/MAGL inhibition

To assess changes in the expression of satellite glial cells in the DRG, as well as astrocytes and microglia in the spinal cord, western blot analyses were conducted following the inhibition of FAAH/MAGL. First, the expression levels of GFAP in satellite glial cells, a type of PNS glial cell, were examined. In the group treated with cisplatin (Cis + Veh), there was a noticeable increase in GFAP expression. However, after JZL195 treatment (Cis + JZL), GFAP expression notably decreased compared to the cisplatin group (Cis + Veh)

(Figure 7A, $F_{2, 15} = 6.274$, $p = 0.0105$, one-way ANOVA followed by Tukey's multiple comparison test). Additionally, changes in microglia in the DRG were analyzed using the Iba1 marker. The expression of Iba1 tended to increase in the group treated with cisplatin (Cis + Veh) and subsequently decrease in the group treated with JZL195 (Cis + JZL). However, the alterations of Iba1 in the DRG were not statistically significant (Figure 7B, $F_{2, 15} = 1.242$, $p = 0.3170$, one-way ANOVA).

The astrocytes, one of the glial cells in the CNS, were also examined by measuring GFAP levels. There was a significant increase in GFAP expression in the group treated with cisplatin (Cis + Veh) compared to the vehicle group (Veh + Veh). In contrast, the group receiving JZL195 (Cis + JZL) exhibited a significant decrease in GFAP expression compared to the cisplatin group (Cis + Veh) (Figure 7C, $F_{2, 15} = 6.949$, $p = 0.0073$, one-way ANOVA followed by Tukey's multiple comparison test). The expression changes of another CNS glial cell, microglia, were assessed using Iba1. The results showed a significant upregulation in Iba1 expression in the spinal cord after cisplatin treatment (Cis + Veh) compared to the group treated with the vehicle (Veh + Veh). However, the increased expression of Iba1 induced by cisplatin decreased after the administration of JZL195 (Cis + JZL) (Figure 7D, $F_{2, 15} = 5.048$, $p = 0.0211$, one-way ANOVA followed by Tukey's multiple comparison test). These findings suggest that the activation of glial cells increased by chemotherapy in the CIPN animal model is alleviated by JZL195, indicating that the inhibition of FAAH/MAGL contributes to relieving pain and neuroinflammation.

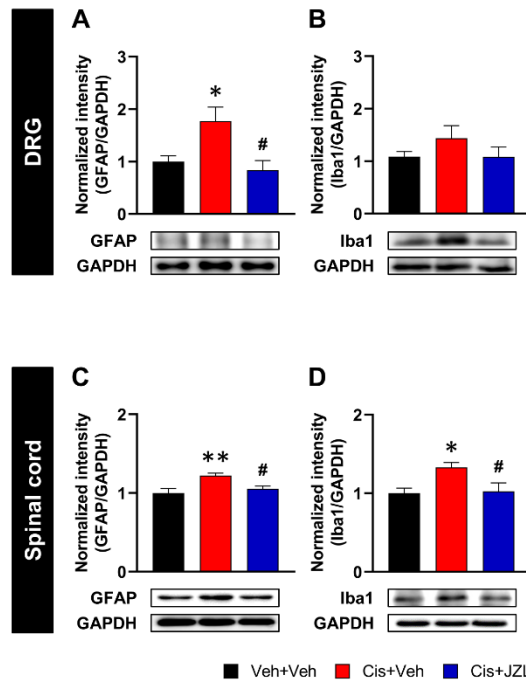


Figure 7. The representative western blot images and quantification of GFAP and Iba1 level in the L4-L6 DRG and spinal cord. (A) The expression of GFAP in Cis + Veh group was significantly increased compared to Veh + Veh group, meanwhile, expression of GFAP in Cis + Veh group was significantly reduced ($n = 6$). (B) The expression of Iba1 was increased by cisplatin and decreased after JZL195. However, alterations of Iba1 in DRG were statistically not significant ($n = 6$). (C) The expression of GFAP in Cis + Veh group was significantly increased compared to Veh + Veh group, meanwhile the expression of Iba1 in Cis + JZL195 group was notably decreased ($n = 6$). (D) The expression of Iba1 in Cis + Veh group was significantly increased compared to Veh + Veh group, meanwhile the expression of Iba1 in Cis + JZL195 group was notably decreased ($n = 6$). Data are presented as mean \pm SEM and analyzed by one-way ANOVA followed by Tukey's multiple comparison test. The significances are marked as * $p < 0.05$ and ** $p < 0.01$, compared with the Veh + Veh group. The significances are marked as # $p < 0.05$, compared with the Cis + Veh group.

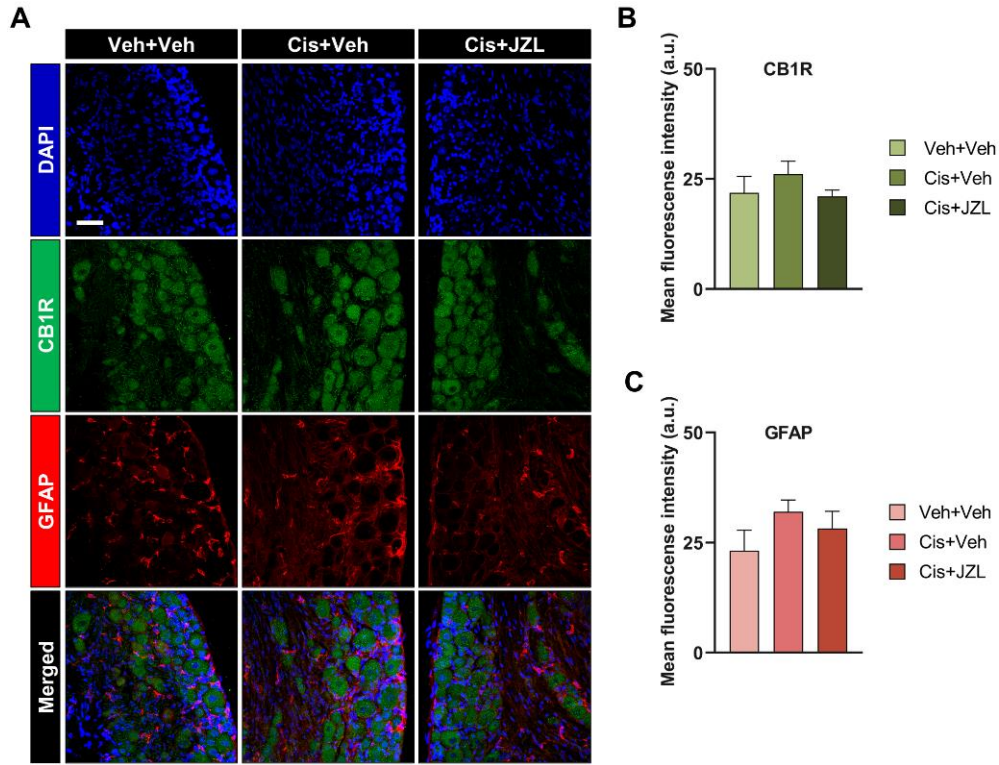
7. Satellite cells in the DRG are regulated by JZL195, along with CB1R, CB2R, and TLR4 expression

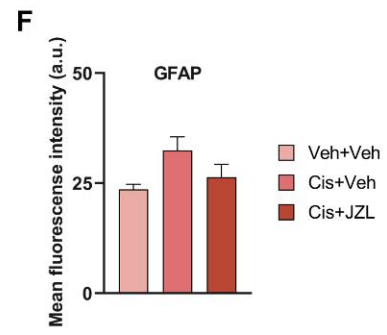
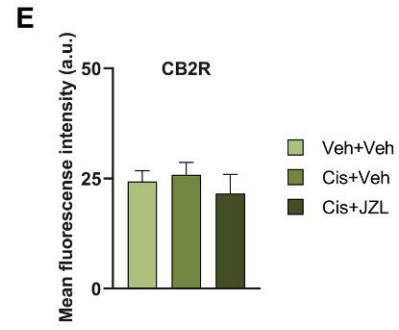
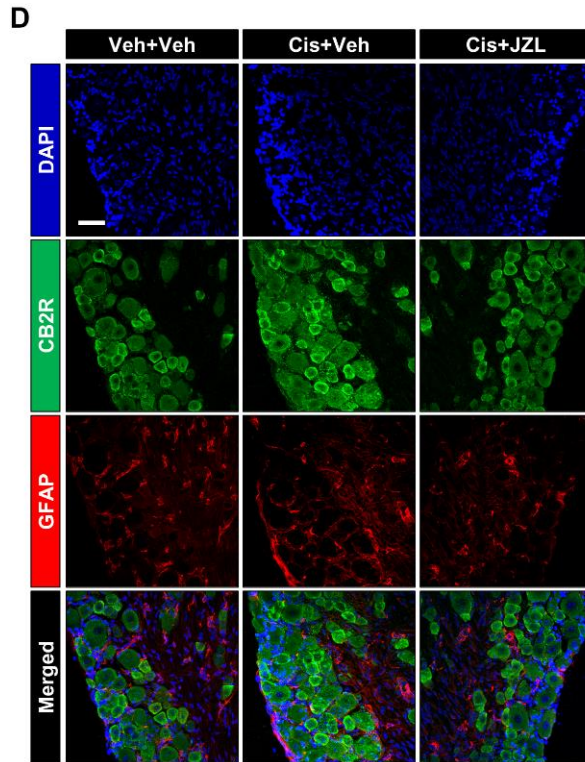
Immunohistochemistry staining was conducted to detect satellite glial cells within the DRG. Changes in the expression of GFAP, a marker specific to satellite glial cells, were observed. Additionally, the presence of CB1R, CB2R, and TLR4 was validated. Immunohistochemistry staining of CB1R and GFAP was conducted in the DRG (Figure 8A). The results revealed a slight increase in mean fluorescence intensity (MFI) of CB1R in the cisplatin group (Cis + Veh) compared to the vehicle group (Veh + Veh). However, upon administration of JZL195 (Cis + JZL), mean fluorescence intensity of CB1R was reduced compared to the cisplatin group (Cis + Veh) (Figure 8B, $F_{2,9} = 0.9120$, $p = 0.4359$, one-way ANOVA). Likewise, GFAP expression appeared to increase after cisplatin administration (Cis + Veh), but JZL195 exhibited a tendency to counteract this upregulation (Cis + JZL) (Figure 8C, $F_{2,9} = 1.354$, $p = 0.3062$, one-way ANOVA).

The mean fluorescence intensity of CB2R was also examined through immunohistochemistry staining along with GFAP (Figure 8D). The mean fluorescence intensity of CB2R showed a slight increase in response to cisplatin treatment (Cis + Veh) but a decrease after JZL195 administration (Cis + JZL) (Figure 8E, $F_{2,9} = 0.4268$, $p = 0.6651$, one-way ANOVA). The mean fluorescence intensity of GFAP showed a similar result to CB2R (Figure 8F, $F_{2,9} = 3.212$, $p = 0.0886$, one-way ANOVA). However, no co-localization was observed between CB2R and GFAP, similar to the earlier findings with CB1R and GFAP. These findings suggest that cannabinoid receptors may play a role in other cell types than glial cells in the DRG. Moreover, the absence of co-localization of cannabinoid receptors with satellite glial cells in the DRG indicates that cannabinoid receptors have a more prominent role in mitigating CIPN in glial cells within the CNS.

The mean fluorescence intensity of TLR4 was also detected along with GFAP (Figure 8G). The mean fluorescence intensity of TLR4 slightly increased after cisplatin injection (Cis +

Veh) and subsequently decreased upon JZL195 treatment (Cis + JZL) (Figure 8H, $F_{2,9} = 0.0192$, $p = 0.9810$, one-way ANOVA). Similarly, the mean fluorescence intensity of GFAP increased after cisplatin administration (Cis + Veh), but it tended to decrease after JZL195 treatment (Cis + JZL) (Figure 8I, $F_{2,9} = 5.845$, $p = 0.0236$, one-way ANOVA followed by Tukey's multiple comparison test). When examining the expression of TLR4 and GFAP simultaneously, no co-localization was observed, indicating that TLR4 may be expressed in different cell types.





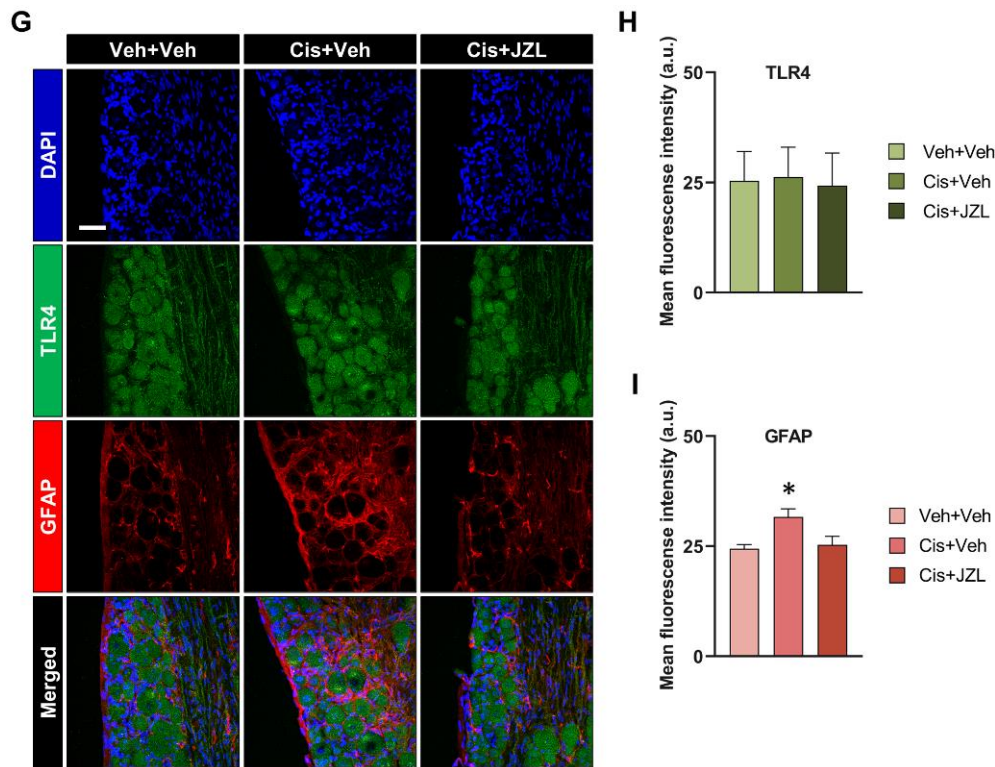


Figure 8. Expression of satellite glial cells with CB1R, CB2R, and TLR4. (A) Representative images of immunohistochemistry staining. CB1R and GFAP in DRG were identified after JZL195 administration. Merged images represented co-localization between CB1R (green) and GFAP (red). (B) The mean fluorescence intensity of CB1R was quantified ($n = 4$). (C) The mean fluorescence intensity of GFAP was quantified ($n = 4$). (D) Representative images of immunohistochemistry staining. CB2R and GFAP in DRG were identified after JZL195 administration. Merged images represented co-localization between CB2R (green) and GFAP (red). (E) The mean fluorescence intensity of CB2R was quantified ($n = 4$). (F) The mean fluorescence intensity of GFAP was quantified ($n = 4$). (G) Representative images of immunohistochemistry staining. TLR4 and GFAP in DRG were identified after JZL195 administration. Merged images

represented co-localization between TLR4 (green) and GFAP (red). (H) The mean fluorescence intensity of TLR4 was quantified ($n = 4$). (I) The mean fluorescence intensity of GFAP was quantified ($n = 4$). The cellular nuclei were stained with DAPI (blue). Scale bar = 50 μm . Data are presented as mean \pm SEM and analyzed by one-way ANOVA followed by Tukey's multiple comparison test. The significances for mean fluorescence intensity of GFAP are marked as $*p < 0.05$, compared with the Veh + Veh group.

8. CB1R, CB2R, and TLR4 co-localized with astrocytes in the spinal cord

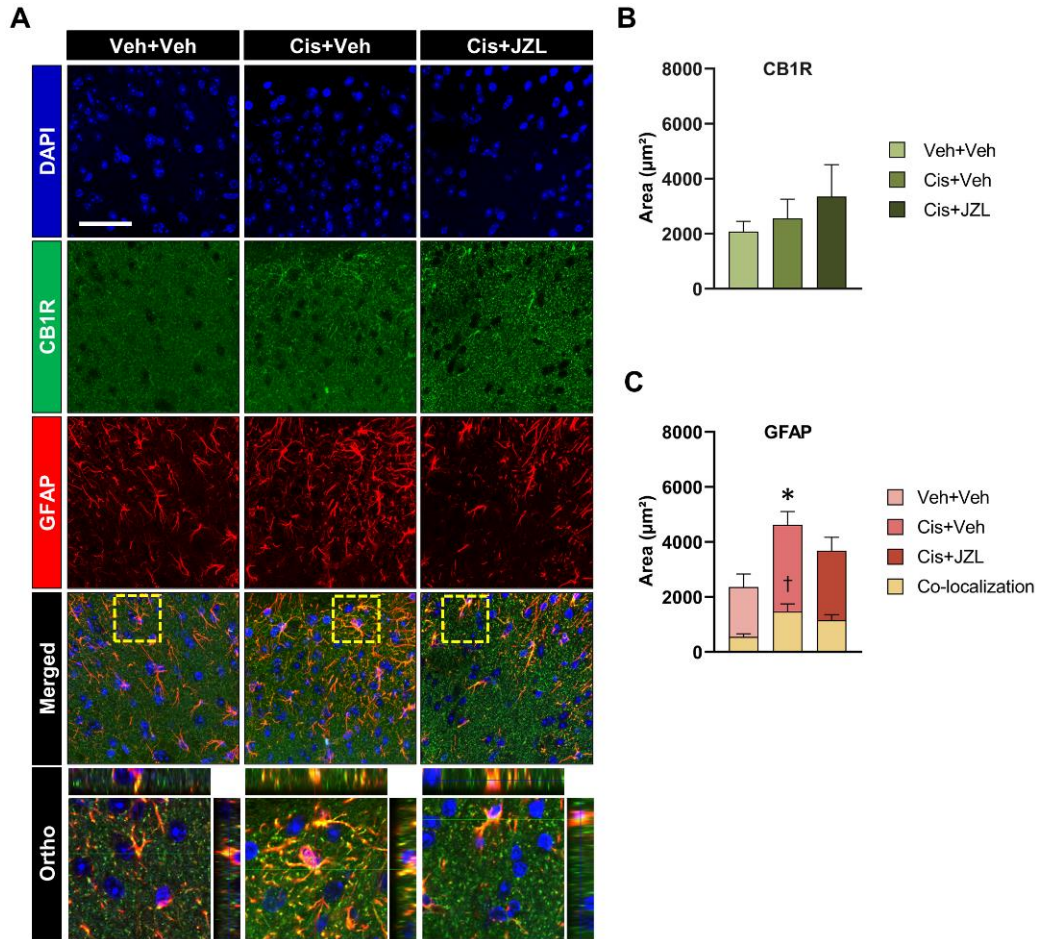
The western blot results in this study confirmed that the expression levels of CB1R, CB2R, and TLR4 in the spinal cord were decreased due to JZL195 treatment. Furthermore, the study aimed to determine whether cannabinoid receptors and TLR4 co-localize with glial cells. Therefore, immunohistochemistry staining of GFAP with cannabinoid receptors or TLR4 was performed to examine the correlation between astrocytes and cannabinoid receptors, as well as TLR4 in the spinal cord (Figure 9A).

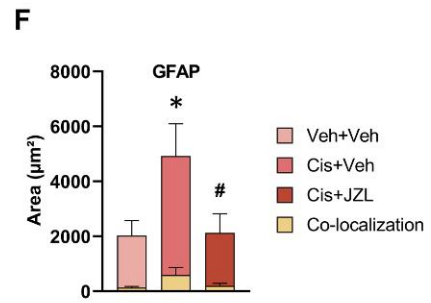
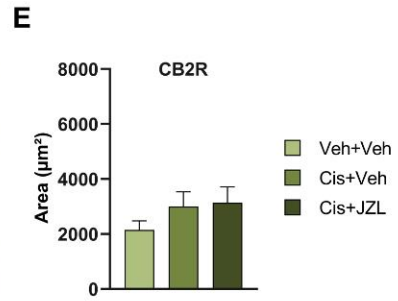
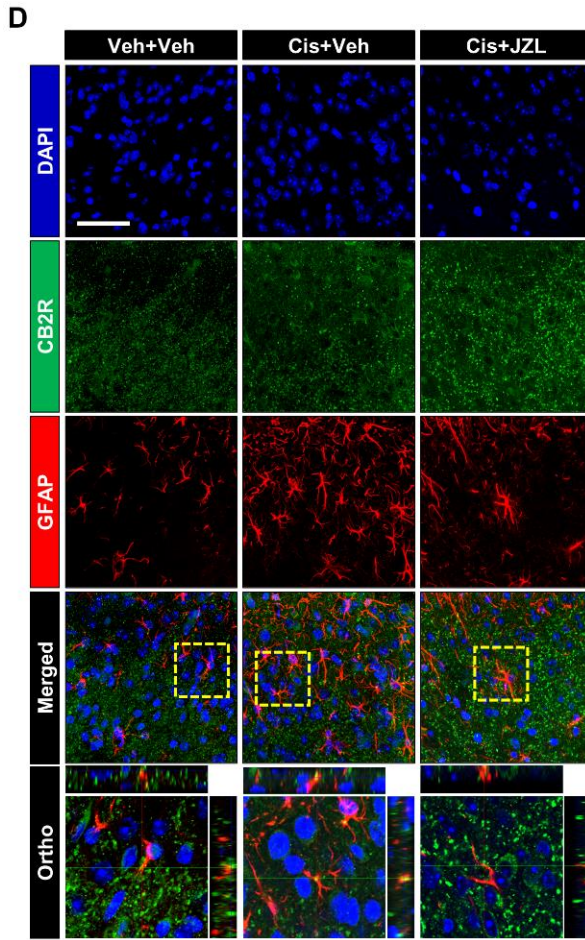
The expression of CB1R was increased due to cisplatin treatment (Cis + Veh) and further upregulated after JZL195 treatment (Cis + JZL). However, these alterations were not statistically significant (Figure 9B, $F_{2, 9} = 0.6364$, $p = 0.5514$, one-way ANOVA). Examination of astrocytes through representative z-stack images revealed a significant increase caused by cisplatin (Cis + Veh) and a subsequent decrease after JZL195 administration (Cis + JZL). Additionally, merged images confirmed the co-localization of CB1R with GFAP, which was increased by cisplatin (Cis + Veh) and then decreased after JZL195 administration (Cis + JZL) (Figure 9C, GFAP, $F_{2, 9} = 4.447$, $p = 0.0454$; co-localization, $F_{2, 9} = 5.055$, $p = 0.0338$, one-way ANOVA followed by Tukey's multiple comparison test). The representative ortho-images demonstrated the expression of CB1R in astrocytes, suggesting that astrocytes could undergo morphological and functional changes by modulating CB1R.

The expression of CB2R was observed through immunohistochemistry staining (Figure 9D). Similar to CB1R, CB2R expression was increased by cisplatin (Cis + Veh) and further upregulated upon JZL195 administration (Cis + JZL). However, the changes in CB2R expression did not reach statistical significance (Figure 9E, $F_{2,9} = 1.153$, $p = 0.3583$, one-way ANOVA). GFAP expression was significantly increased by cisplatin (Cis + Veh) and notably decreased after JZL195 administration (Cis + JZL). The co-localization of CB2R with GFAP was confirmed through merged images, demonstrating that CB2R was co-localized with GFAP (Figure 9F, GFAP, $F_{2,9} = 7.532$, $p = 0.012$; co-localization, $F_{2,9} = 2.980$, $p = 0.1016$, one-way ANOVA followed by Tukey's multiple comparison test).

Finally, to determine the relationship between TLR4 and cannabinoid receptors in astrocytes, immunohistochemistry staining of TLR4 and GFAP were performed (Figure 9G). Representative z-stack images showed that TLR4 expression was increased by cisplatin (Cis + Veh), and the upregulated TLR4 expression was again reduced by JZL195 (Cis + JZL). However, these differences were not statistically significant (Figure 9H, for TLR4: $F_{2,9} = 0.4557$, $p = 0.6478$, one-way ANOVA). Furthermore, GFAP expression was significantly increased by cisplatin (Cis + Veh) and reduced after JZL195 administration (Cis + JZL) (Figure 9I, GFAP, $F_{2,9} = 4.601$, $p = 0.042$; co-localization, $F_{2,9} = 2.335$, $p = 0.1525$, one-way ANOVA followed by Tukey's multiple comparison test). The merged images showed that TLR4 co-localized with GFAP.

These findings, demonstrating the presence of both CB1R and TLR4 within astrocytes, suggest a potential correlation and regulatory interaction between CB1R and TLR4 in astrocytes.





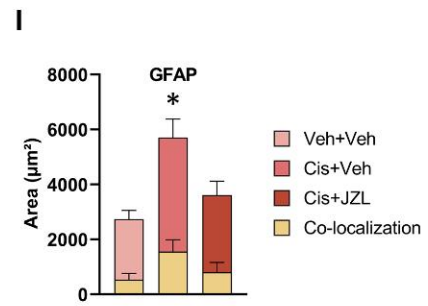
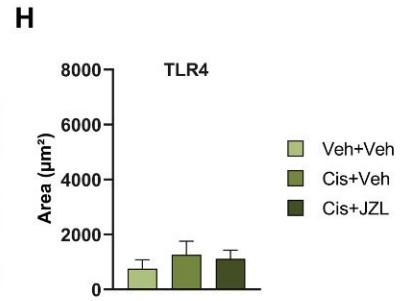
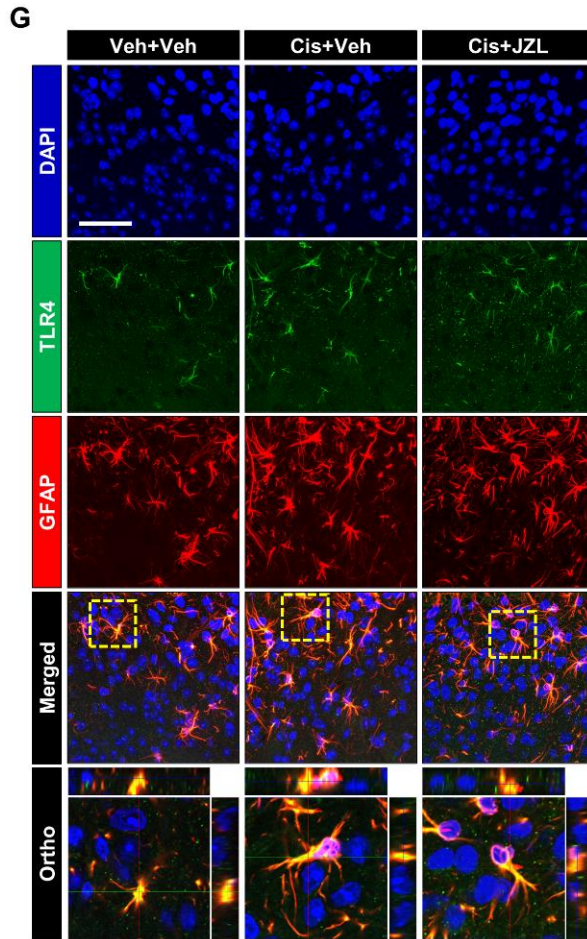


Figure 9. Co-localization of CB1R, CB2R, and TLR4 expression with astrocytes. (A) Representative images of immunohistochemistry staining. CB1R and GFAP in dorsal horn of the spinal cord were identified after JZL195 administration. Merged and ortho images represented co-localization between CB1R (green) and GFAP (red) by yellow. (B) The quantification of CB1R expression area (n = 4). (C) The quantification of GFAP expression area and co-localization area (n = 4). (D) Representative images of immunohistochemistry staining. CB2R and GFAP in dorsal horn of the spinal cord were identified after JZL195 administration. Merged and ortho images represented co-localization between CB2R (green) and GFAP (red) by yellow. (E) The quantification of CB2R expression area (n = 4). (F) The quantification of GFAP expression area and co-localization area (n = 4). (G) Representative images of immunohistochemistry staining. TLR4 and GFAP in dorsal horn of the spinal cord were identified after JZL195 administration. Merged and ortho images represented co-localization between TLR4 (green) and GFAP (red) by yellow. (H) The quantification of TLR4 expression area (n = 4). (I) The quantification of GFAP expression area and co-localization area (n = 4). The cellular nuclei were stained with DAPI (blue). Scale bar = 50 μ m. Data are presented as mean \pm SEM and analyzed by one-way ANOVA followed by Tukey's multiple comparison test. The significances for GFAP area are marked as *p < 0.05, compared with the Veh + Veh group and #p < 0.05, ##p < 0.01, compared with the Cis + Veh group. The significance for co-localized area is marked as †p < 0.05, compared with the Veh + Veh group.

9. CB1R, CB2R, and TLR4 co-localized with microglia in the spinal cord

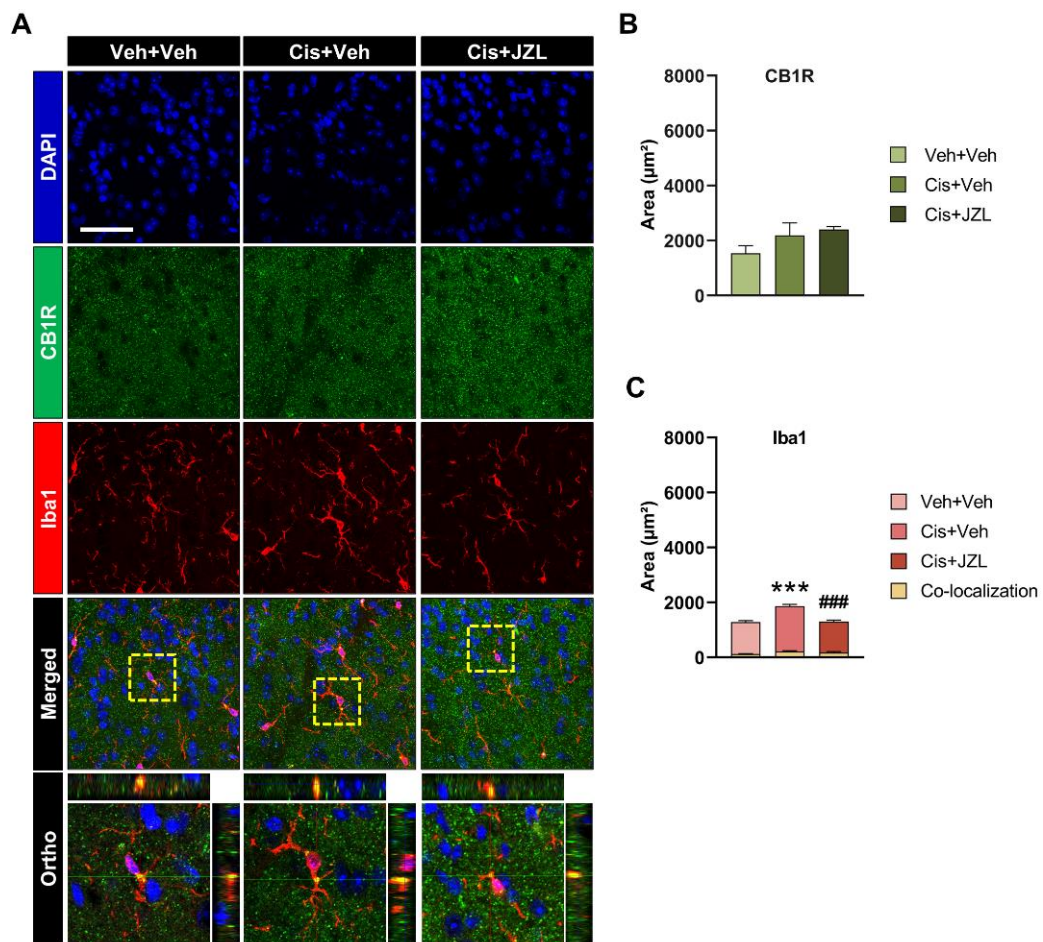
The immunohistochemistry staining was performed to investigate the changes in expression of CB1R, CB2R, TLR4, and microglia following FAAH/MAGL inhibition and to identify co-localization between microglia and receptors (Figure 10A).

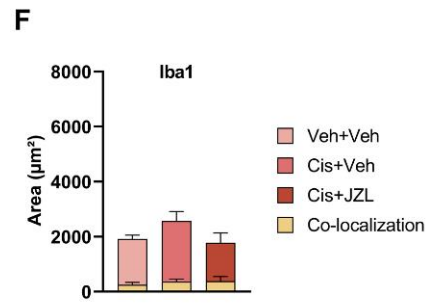
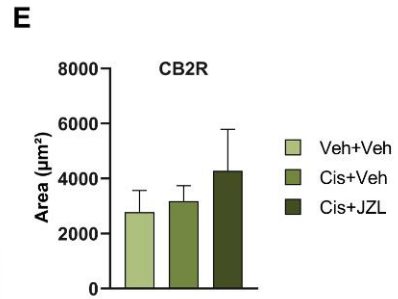
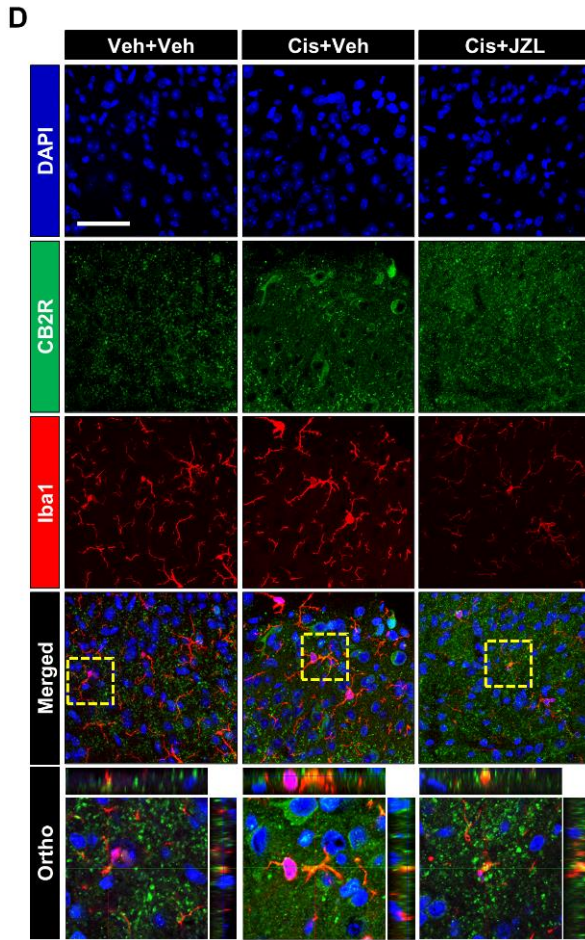
The expression of CB1R in the spinal cord was increased by cisplatin (Cis + Veh) and further elevated after administering JZL195 (Cis + JZL). However, the alteration of CB1R expression was not statistically significant (Figure 10B, $F_{2,9} = 0.9845$, $p = 0.4105$, one-way ANOVA). In contrast, Iba1 was significantly activated by cisplatin (Cis + Veh), but notably attenuated after JZL195 administration (Cis + JZL) (Figure 10C, GFAP, $F_{2,9} = 33.77$, $p < 0.0001$; co-localization, $F_{2,9} = 1.941$, $p = 0.1992$, one-way ANOVA followed by Tukey's multiple comparison test). Furthermore, ortho images showed that CB1R co-localized with Iba1. This indicates the presence of CB1R in microglia, suggesting that microglia may be morphologically and functionally regulated by CB1R.

The expression of CB2R was observed through immunohistochemistry staining (Figure 10D). CB2R expression changed similarly to CB1R after the administration of cisplatin and JZL195 (Figure 10E, $F_{2,9} = 0.5472$, $p = 0.5967$, one-way ANOVA). In addition, the expression of Iba1 was elevated by cisplatin (Cis + Veh) and attenuated after JZL195 treatment (Cis + JZL). However, these changes were not statistically significant (Figure 10F, GFAP, $F_{2,9} = 1.452$, $p = 0.2841$; co-localization, $F_{2,9} = 0.4573$, $p = 0.6469$, one-way ANOVA). Additionally, the merged images revealed that CB2R co-localized with Iba1, indicating the potential modulation of microglia by CB2R.

To investigate the potential association between cannabinoid receptors and TLR4 expressed in microglia, immunohistochemistry staining was conducted (Figure 10G). The representative images revealed an increase in TLR4 expression due to cisplatin treatment (Veh + Cis) and a subsequent decrease after JZL195 administration (Cis + JZL) (Figure 10H, $F_{2,9} = 0.7293$, $p = 0.5087$, one-way ANOVA). The expression of Iba1 was increased by cisplatin (Cis + Veh) and reduced by JZL195 (Cis + JZL). However, these differences

were not significant (Figure 10I, GFAP, $F_{2,9} = 0.8830$, $p = 0.4465$; co-localization, $F_{2,9} = 1.193$, $p = 0.3471$, one-way ANOVA). In addition, representative ortho images confirmed that TLR4 was co-localized with Iba1. These findings indicate that CB1R, CB2R, and TLR4 are present in microglia, suggesting that cannabinoid receptors could be associated with TLR4.





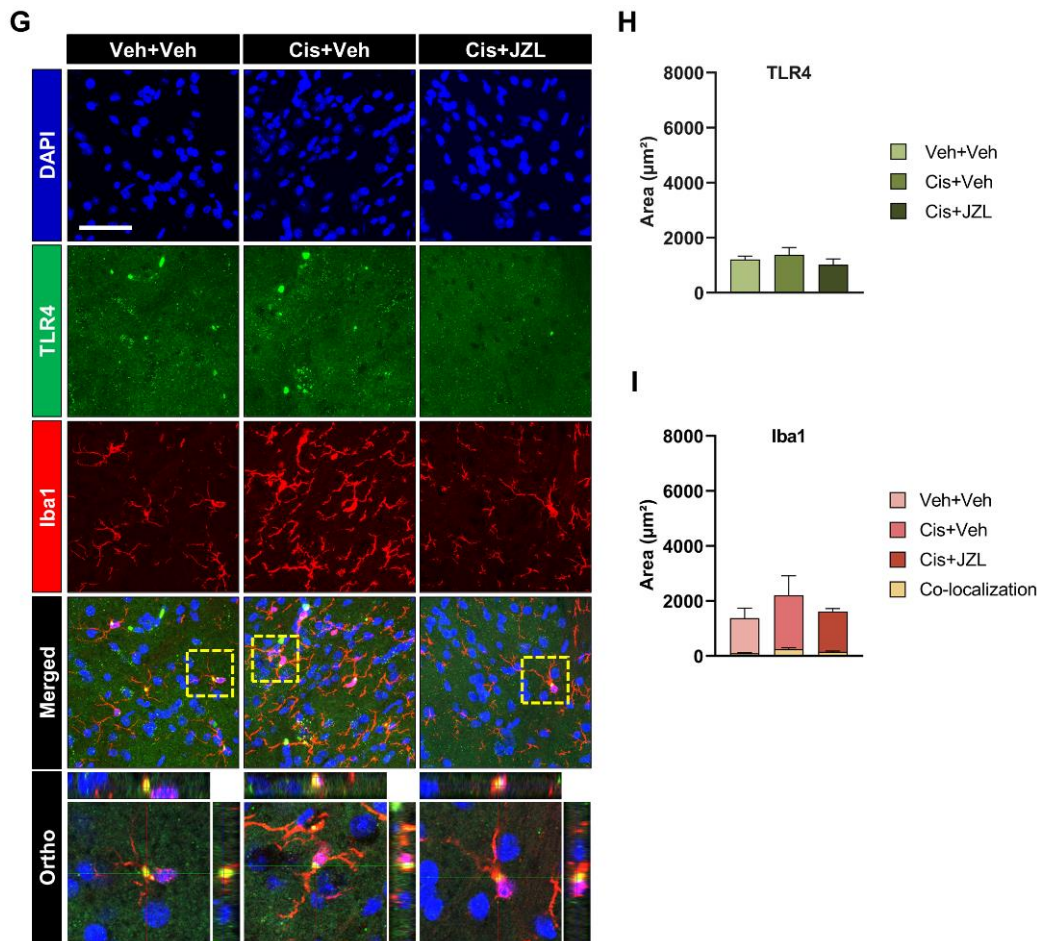


Figure 10. Co-localization of CB1R, CB2R, and TLR4 expression with microglia. (A) Representative images of immunohistochemistry staining. CB1R and Iba1 in dorsal horn of the spinal cord were identified after JZL195 administration. Merged and ortho images represented co-localization between CB1R (green) and Iba1 (red) by yellow. (B) The quantification of CB1R expression area (n = 4). (C) The quantification of Iba1 expression area and co-localization area (n = 4). (D) Representative images of immunohistochemistry staining. CB2R and Iba1 in dorsal horn of the spinal cord were identified after

JZL195 administration. Merged and ortho images represented co-localization between CB2R (green) and Iba1 (red) by yellow. (E) The quantification of CB2R expression area (n = 4). (F) The quantification of Iba1 expression area and co-localization area (n = 4). (G) Representative images of immunohistochemistry staining. TLR4 and Iba1 in dorsal horn of the spinal cord were identified after JZL195 administration. Merged and ortho images represented co-localization between TLR4 (green) and Iba1 (red) by yellow. (H) The quantification of TLR4 expression area (n = 4). (I) The quantification of Iba1 expression area and co-localization area (n = 4). The cellular nuclei were stained with DAPI (blue). Data are presented as mean \pm SEM and analyzed by one-way ANOVA followed by Tukey's multiple comparison test. Scale bar = 50 μ m. The significances for Iba1 area are marked as * $p < 0.05$, compared with the Veh + Veh group and ### $p < 0.001$, compared with the Cis + Veh group.

10. Two types of cannabinoid receptors act similarly on pain-relief effects

To evaluate the pharmacological effects of JZL195 on the CNS, AM251 and AM630, antagonists of CB1R and CB2R, respectively, were injected intrathecally at a concentration of 0.01 mg/kg and 0.03 mg/kg. As in the present study, cisplatin was used to develop a CIPN model, and the mechanical allodynia was evaluated by determining the 50% withdrawal thresholds (Figure 11A, for days: $F_{4, 112} = 154.0$, $p < 0.0001$; for groups: $F_{4, 28} = 0.3118$, $p = 0.8677$; for days \times groups interaction: $F_{16, 112} = 0.5253$, $p = 0.9289$, two-way ANOVA). On day 14, 0.01 mg/kg AM251 displayed a slight tendency to decrease the 50% withdrawal thresholds, which were increased by JZL195, but this effect did not reach statistical significance. Conversely, 0.01 mg/kg AM630 significantly decreased the 50% withdrawal thresholds, counteracting the effects of JZL195. When the dose of AM251 was increased to 0.03 mg/kg, it significantly decreased the 50% withdrawal thresholds, in contrast to the insignificant effect observed at 0.01 mg/kg. Similarly, AM630 at 0.03 mg/kg

also significantly reduced the 50% withdrawal thresholds, demonstrating greater inhibition of JZL195 compared to the 0.01 mg/kg dose (Figure 11B, for time: $F_{4, 112} = 25.53$, $p < 0.0001$; for groups: $F_{4, 28} = 1.088$, $p = 0.3813$; for time \times groups interaction: $F_{16, 112} = 1.264$, $p = 0.2327$, two-way ANOVA followed by Bonferroni's multiple comparison test). The responses to acetone were also measured using the acetone test to confirm the cold allodynia induced by cisplatin (Figure 11C, for days: $F_{4, 112} = 46.38$, $p < 0.0001$; for groups: $F_{4, 28} = 0.2816$, $p = 0.8874$; for days \times groups interaction: $F_{16, 112} = 0.9235$, $p = 0.5447$, two-way ANOVA). Subsequently, the same concentrations of AM251 and AM630 used in the up-down test were administered to evaluate their effect on counteracting JZL195. The results showed that AM251 and AM630 at 0.01 mg/kg slightly increased the responses to acetone, which were reduced by JZL195, but the difference was not statistically significant. In contrast, when AM251 and AM630 were administered at 0.03 mg/kg, they significantly enhanced the responses to acetone, indicating that they effectively counteracted the pain-relieving effects of JZL195 (Figure 11D, for time: $F_{4, 112} = 19.20$, $p < 0.0001$; for groups: $F_{4, 28} = 0.4854$, $p = 0.7463$; for time \times groups interaction: $F_{16, 112} = 1.124$, $p = 0.3421$, two-way ANOVA followed by Bonferroni's multiple comparison test). These findings indicated that when low concentrations of the antagonists were administered, CB2R appeared to have a more significant influence on regulating mechanical allodynia. Conversely, when high concentrations of the antagonist were used, CB1R seemed to have a more pronounced role in mechanical allodynia. Additionally, the results suggest that both CB1R and CB2R play equally significant roles in pain relief during cold allodynia.

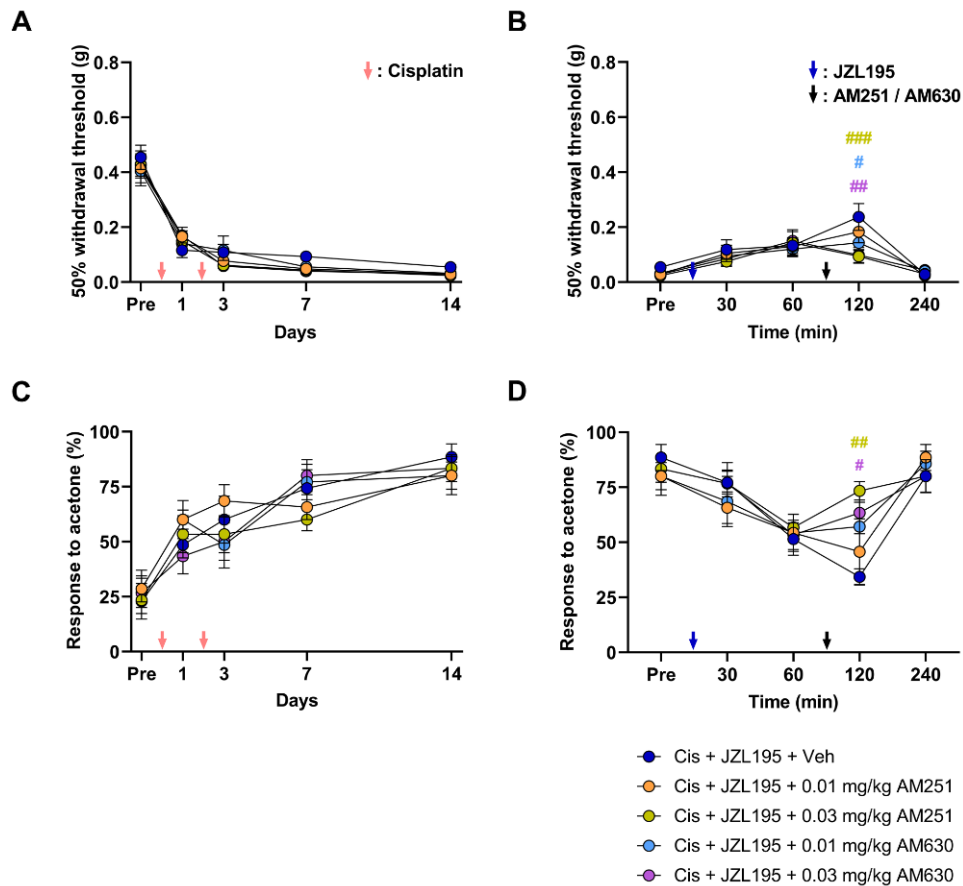


Figure 11. Assessment of the mechanical allodynia and cold allodynia after administrating antagonists for cannabinoid receptors. (A) Development of the mechanical allodynia after cisplatin injection. Cisplatin groups (Cis + JZL195 + Veh, Cis + JZL195 + 0.01 mg/kg AM251, and Cis + JZL195 + 0.01 mg/kg AM630; n = 7, Cis + JZL195 + 0.03 mg/kg AM251 and Cis + JZL195 + 0.03 mg/kg AM630; n = 6) showed decrease in the 50% withdrawal thresholds from day 1 to day 14. (B) The pain-relieving effect of JZL195 on the mechanical allodynia was inhibited by AM251 and AM630. Intrathecal injection of 0.01 mg/kg of AM630, 0.03 mg/kg of AM251, and 0.03 mg/kg of AM630 significantly decreased 50%

withdrawal thresholds which were alleviated by JZL195. (C) Development of cold allodynia after cisplatin injection. Cisplatin-treated groups (Cis + JZL195 + Veh, Cis + JZL195 + 0.01 mg/kg AM251, and Cis + JZL195 + 0.01 mg/kg AM630; n = 7, Cis + JZL195 + 0.03 mg/kg AM251 and Cis + JZL195 + 0.03 mg/kg AM630; n = 6) showed increase in the responses to acetone from day 1 to day 14. (D) The pain-relieving effect of JZL195 on cold allodynia was inhibited by AM251 and AM630. Intrathecal injection of 0.03 mg/kg of AM251 and 0.03 mg/kg of AM630 significantly increased the responses to acetone, which were mitigated by JZL195. Data are presented as mean \pm SEM and analyzed by two-way ANOVA followed by Bonferroni's post hoc multiple comparison test. The significances are marked as # $p < 0.05$, ## $p < 0.01$, and ### $p < 0.001$, compared with the Cis + JZL195 + Veh group.

11. JZL195 did not affect locomotor activity as well as pain-related behavior in normal mice

To determine whether JZL195 affects locomotor-related behavior in normal mice, we measured total distance and movement time using the OFT. Total distance represents the cumulative distance traveled by the mice, while movement time indicates the duration of their activity. The results revealed no difference in total distance between the normal group and the vehicle group, which was treated with DMSO in ethanol, cremophor, and sterile normal saline (1:1:18). However, the JZL195 group, which received a dosage of 20 mg/kg of JZL195, exhibited a slight decrease in total distance 2 h after JZL195 injection, although this decrease was not statistically significant. At 24 h after JZL195, JZL195 group showed a slight increase in total distance, with no statistically significant difference among the three groups (Figure 12A and B, 0 h, $p = 0.2475$; 2 h, $p = 0.5381$; 24 h, $p = 0.7596$, one-way ANOVA). Similarly, movement time of the JZL195 group showed a tendency to decrease 2 h after injection, but this effect was not statistically significant. After 24 h, there was no

significant difference in movement time among the three groups (Figure 12C, 0 h, $p = 0.7761$; 2 h, $p = 0.5622$; 24 h, $p = 0.9549$, one-way ANOVA). These findings suggest that JZL195 has the potential to affect locomotor activity in normal mice 2 h after administration, but these effects diminish after 24 h.

To determine the effect of JZL195 on mechanical allodynia, the up-down test was performed in time dependent manner. Pain-related behavioral changes were observed at 0, 0.5, 1, 2, 4, 8, 12, and 24 h after administration of 20 mg/kg JZL195. However, the behavioral tests conducted on the three groups did not show any statistically significant changes over time (Figure 12D, for time: $F_{8, 144} = 1.737$, $p = 0.0947$; for groups: $F_{2, 18} = 0.5955$, $p = 0.5618$; for time \times groups interaction: $F_{16, 144} = 0.4869$, $p = 0.9503$, two-way ANOVA). These findings indicate that JZL195 does not affect pain-related behaviors in normal mice.

To assess the potential impact of JZL195 on the body weight of normal mice, the body weights were measured before and after the administration of JZL195. The results revealed no significant difference in body weight among the three groups after JZL195 administration, indicating that JZL195 does not have a substantial impact on body weight (Figure 12E, for time: $F_{2, 36} = 17.81$, $p < 0.0001$; for groups: $F_{2, 18} = 2.804$, $p = 0.0871$; for time \times groups interaction: $F_{4, 36} = 0.5065$, $p = 0.7312$, two-way ANOVA).

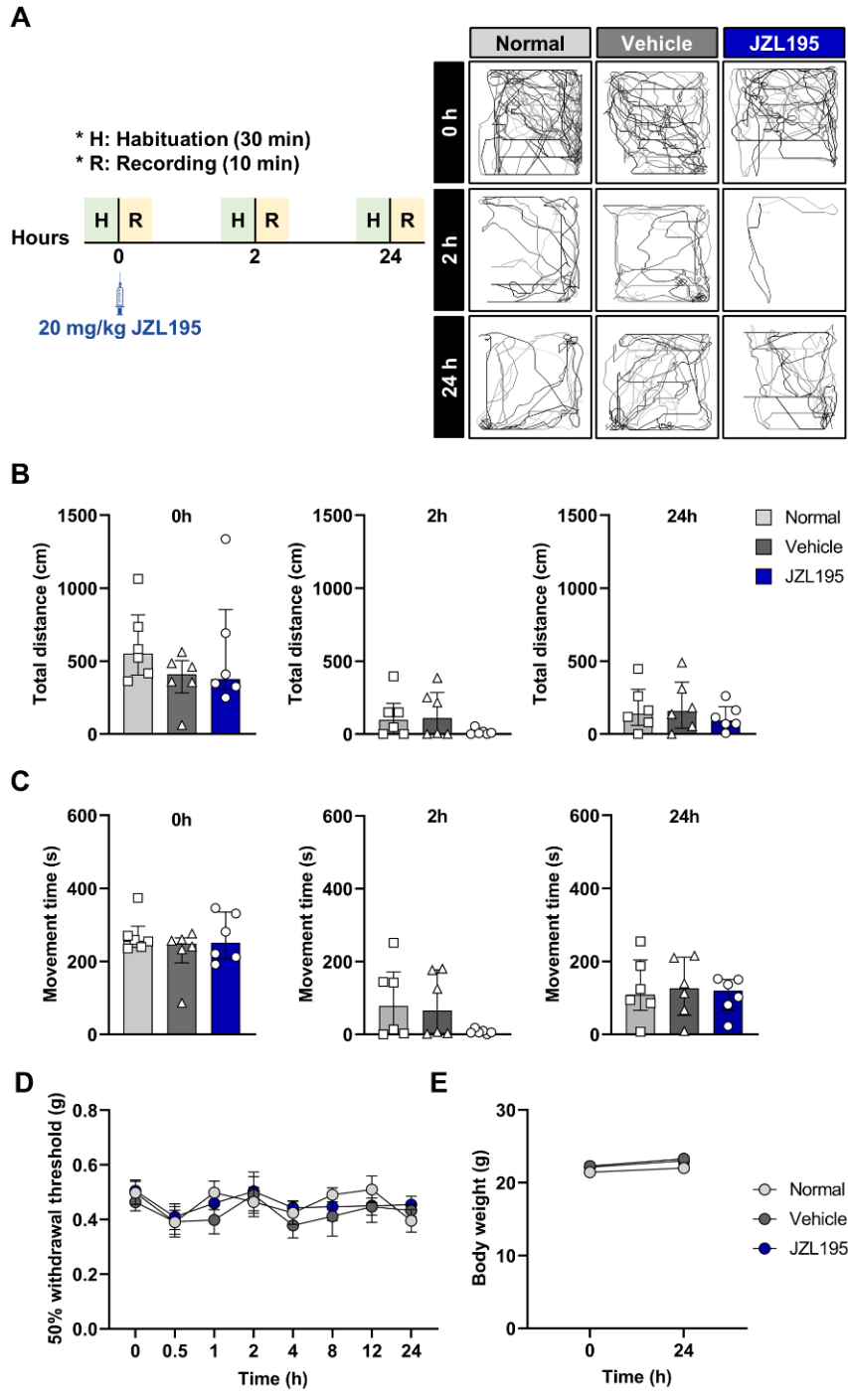


Figure 12. Effect of the JZL195 on locomotor activity and withdrawal thresholds in normal mice. (A) An illustration of experimental timeline for OFT and a representative pattern of the distance traveled by mice in three groups. The groups are divided into a group that received no treatment (normal group; n = 6), a group that received vehicle as a control for JZL195 (vehicle group; n = 6), and a group that received 20 mg/kg of JZL195 (JZL195 group; n = 6). At 2 h, the movement patterns of the three groups were generally reduced compared to 0 h, with the JZL195 group exhibiting less mobility than the normal and vehicle groups. At 24 h, the movement patterns of mice in all three groups increased compared to 2 h, and these patterns were similar across the groups. (B) Measurements of the total distance traveled by the mice in three groups. The total distance traveled by the mice tended to decrease at 2 h than 0 h. However, there was no significant difference in the total distance traveled among the three groups at 2 h. Furthermore, at the 24 h, the total distance traveled remained consistent with the measurements taken at 2 h, with no significant variations observed among the three groups. (C) Measurements of the time that mice have traveled. Movement time of the mice tended to decrease at 2 h compared to 0 h, but there was no significant difference between the three groups at either 0 or 2 h. Movement time measured at 24 h tended to be slightly increased than at 2 h, with no significant difference between the three groups. Data are presented as median with IQR and analyzed by one-way ANOVA and Kruskal-Wallis non-parametric tests. (D) Changes in 50% withdrawal thresholds in normal mice. The 50% withdrawal thresholds exhibited no significant alterations among the three groups. (E) Changes in body weight in the normal mice. The body weight did not demonstrate significant variances between the three groups. Data are presented as mean \pm SEM and analyzed by two-way ANOVA followed by Bonferroni's post hoc multiple comparison test.

IV. DISCUSSION

CIPN is a multifactorial adverse effect that arises after chemotherapy and is characterized by sensorimotor dysfunction in the distal extremities, as well as alterations in factors associated with neuroinflammation. The aim of this study was to investigate how JZL195, a dual FAAH/MAGL inhibitor, affects cannabinoid receptors and TLR4 in glial cells, along with inflammatory cytokines that are involved in pain processing and neuroinflammatory responses, in a CIPN animal model. First, mechanical allodynia and cold allodynia were examined on day 7 and day 14 and locomotor activities were examined on day 8 and day 15 following the development of CIPN by cisplatin. Subsequently, further experiments were conducted on day 14. On day 14, the animal model of CIPN received three different concentrations of JZL195. 2 h after administering JZL195, a concentration of 20 mg/kg was found to be the most effective in alleviating both mechanical and cold allodynia without significantly affecting locomotor activity. Furthermore, western blot and immunohistochemistry staining revealed that the activity of ECS and glial cells, as well as TLR4 expression, increased upon cisplatin treatment, while glial cell activity and TLR4 levels decreased after JZL195 administration. In particular, the expressions of cannabinoid receptors were differentially regulated in the DRG and spinal cord by JZL195. Immunohistochemistry staining was conducted to verify the co-localization of cannabinoid receptors with TLR4 in glial cells within the DRG and spinal cord. The results showed that satellite glial cells in the DRG did not co-localize with neither cannabinoid receptor nor TLR4, while cannabinoid receptors co-localized with glial cells in the spinal cord, along with TLR4. Notably, the present study demonstrates a positive correlation between CB1R and TLR4 in glial cells of the spinal cord in the CIPN animal model.

1. The animal model of CIPN exhibits different locomotor activities depending on the development stage

CIPN is primarily associated with sensory nerve disorders, making it important to assess motor responses when evaluating CIPN.^{59,60} Behavioral alterations often rely on motor responses, emphasizing the need to confirm the absence of motor deficits.⁵⁰ Additionally, assessing motor responses is vital because high doses of certain drugs can cause both sensory alteration and motor impairment.⁶¹ Therefore, this study not only assessed pain through the up-down test and acetone test, but also measured locomotor activities using the OFT to establish a CIPN model that exhibits similar behavior to previous studies with minimal cisplatin administration.

In this study, an animal model of CIPN was established by administering cisplatin twice. The mechanical and cold allodynia were assessed up to day 7 or day 14 following cisplatin administration. To gain a better understanding of the different stages of CIPN development by evaluating motor responses, the locomotor activities of the mice were also monitored and measured to compare the results between day 8 and day 15. The results indicated that both mechanical and cold allodynia persisted until day 7 or day 14. The total distance and movement time were significantly longer in the cisplatin group compared to the vehicle group on day 8, while no significant difference was observed between the vehicle and cisplatin groups on day 15.

These findings contrast with previous research that measured locomotor activity after cisplatin administration. In the study of cognitive impairment, the cisplatin group demonstrated a significant decrease in distance traveled compared to the control group.⁶² Another study using cisplatin showed a significant decrease in the total distance traveled by both male and female rats treated with cisplatin, compared to their corresponding control groups.⁶³ Conversely, the outcomes of the OFT in the prior CIPN investigation exhibited similarities to our findings. In the CIPN study, it was observed that the group treated with cisplatin traveled a significantly longer distance than the control group during the early

time points (days 5 and 6). However, this difference decreased during the later time points (days 20 and 21).⁵⁰ Based on this study, this study found that the results at day 15 closely mirrored those observed at the later time point. Therefore, day 14 was chosen for further experiments.

2. Inhibition of FAAH/MAGL alleviates chemotherapy-induced peripheral neuropathy

Research on cannabis-derived drugs can be categorized into two groups. In one group, the agonist directly interacts with cannabinoid receptors to produce therapeutic effects, while in the other, the drug indirectly affects cannabinoid receptors. This indirect effect may involve targeting catabolic enzymes to inhibit them, thereby increasing endocannabinoid levels and resulting in therapeutic effects.⁴⁴⁻⁴⁶ However, direct action of cannabis-derived drugs on cannabinoid receptors, particularly CB1Rs, carries the risk of psychoactive side effects. Despite these drawbacks, it is worth noting that CB1Rs are more abundant in the body than CB2Rs, indicating a more substantial role in pain regulation.⁴⁶ Therefore, this research aimed to alleviate CIPN through the use of JZL195, which could indirectly influence both CB1R and CB2R by increasing AEA and 2-AG levels through FAAH and MAGL inhibition. JZL195 has previously been shown to relieve various types of pain including inflammatory pain, neuropathic pain, and migraine pain.^{48,49,64} In this study, analgesic effect of JZL195 on CIPN-related pain were assessed. The findings of this study demonstrate that the administration of JZL195, a dual FAAH/MAGL inhibitor, alleviates peripheral neuropathy in an animal model of CIPN.

As this is the first study to use JZL195 in a CIPN animal model, the first step in this study was to determine the optimal concentration of JZL195 to produce pain relief in the CIPN animal model. In a study of restraint stress-induced analgesia, subcutaneous administration of 10 mg/kg of JZL195 was found to induce a significant increase in hot-plate latency and paw withdrawal latency (PWL), which were also increased by restraint stress.⁵¹ In a recent

study on sporadic dementia, oral administration of 20 mg/kg JZL195 for 15 days led to a reduction in IL-6 and TNF- α levels, with no significant alterations in locomotor activity or neurobehavioral impairment.⁵² Based on these studies, three different concentrations were established as low (3 mg/kg), medium (10 mg/kg), and high (20 mg/kg).

Behavioral tests were then used to assess the analgesic effect of JZL195 over time and determine which of the three concentrations had the greatest effect. As a results, 20 mg/kg of JZL195 successfully ameliorated both mechanical and cold allodynia after 2 h, while having no impact on locomotor activity. In line with the present study, JZL195 has shown pain relief effects in other animal models. In an inflammatory pain model study, subcutaneous injection of JZL195 reduced mechanical allodynia at concentrations above 3 mg/kg and reduced thermal hyperalgesia at concentrations above 20 mg/kg.⁴⁹ Similarly, in the neuropathic pain model, subcutaneous administration of JZL195 reduced mechanical and cold allodynia.⁴⁸ These results demonstrate that JZL195 can effectively reduce inflammatory pain, neuropathic pain, as well as mechanical and cold allodynia related to CIPN. However, JZL195 is also known to affect locomotor activity.⁶⁵ In the inflammatory pain model study, 20 and 30 mg/kg of JZL195 reduced crossing number in the OFT.⁴⁹ The findings from the mood and anxiety study contradicted those of the inflammatory pain study. 2 h after the systemic administration of 40 mg/kg JZL195, the JZL195-treated group traveled notably farther than the control group.⁶⁵ These differences suggest that JZL195 likely has varying effects on pain-related behavior and locomotor activity depending on the concentration used. Hence, this implies the crucial need to select the appropriate concentration of JZL195 based on the specific purpose to be achieved.

3. The ECS in the DRG and spinal cord of the CIPN animal model is differentially regulated

The endocannabinoids have a short bioavailability due to rapid degradation by catabolic enzymes.⁶⁶ As a result, the ECS undergoes various regulatory mechanisms depending on

the specific pathological condition. Multiple studies on CIPN have demonstrated alterations in the activity of the ECS within the DRG and spinal cord after receiving chemotherapeutic agents.⁶⁷⁻⁷⁰ However, no studies have identified how the ECS is regulated in the DRG and spinal cord after simultaneously inhibiting FAAH and MAGL in an animal model of CIPN. Therefore, this study sought to elucidate alterations of the ECS in the DRG and spinal cord induced by JZL195 treatment and to understand these changes in conjunction with behavioral tests.

Western blot analysis revealed an increase in the levels of two catabolic enzymes in both the DRG and spinal cord after cisplatin treatment. Similar alterations in FAAH or MAGL expression in the DRG or spinal cord have been confirmed by several studies. Previous pain research has reported increased FAAH expression in the DRG of rats that underwent sciatic nerve surgery.⁷¹ In addition, in a study on neuropathic pain, the group that received chronic constriction injury to the sciatic nerve exhibited a significant increase in MAGL immunofluorescent intensity compared to the group that underwent a sham injury.⁷² However, these previous studies have limitations in comprehensively evaluating alterations in the endocannabinoid system, as they do not demonstrate changes in both FAAH and MAGL expression in both the DRG and spinal cord. Therefore, it is important to note that this study differs from previous ones as it identifies changes in the expression of both FAAH and MAGL in both the DRG and spinal cord of the CIPN animal model. Moreover, this investigation revealed alterations in FAAH and MAGL expression after JZL195 administration. Western blot analysis verified that JZL195 treatment leads to a reduction in FAAH and MAGL expression, aligning with findings from previous research. Earlier research has demonstrated that the expression of FAAH and MAGL is inhibited in a concentration-dependent manner following intraperitoneal administration of JZL195.⁴⁷

Interestingly, the results of this study revealed differences in the expression of cannabinoid receptors in the spinal cord compared to the expression of catabolic enzymes. Following cisplatin administration, the expression of CB1R and CB2R increased, but the changes were not significant. Conversely, after JZL195 administration, the expression of

CB1R and CB2R increased, while the expression of FAAH and MAGL decreased. Remarkably, the expression of cannabinoid receptors in the DRG and spinal cord exhibited a different pattern following the administration of JZL195, as the expression of cannabinoid receptors in the DRG was significantly reduced. These findings imply distinct regulatory mechanisms for cannabinoid receptors in specific regions. These results align with what has been observed in animal models and cases of human disease, indicating that the signaling in the ECS is regulated differently in a tissue-specific manner.⁷³ The expression of cannabinoid receptors has also been examined in other pain models. In a study on neuropathic pain, findings revealed a significant upregulation of CB2R expression in the DRG of the nerve injury group at 21 days after surgery compared to the sham injury group.⁷⁴ Meanwhile, a spinal cord injury (SCI) model study reported a significant increase in CB2R expression from 3 days to 2 weeks after SCI surgery, followed by a gradual decrease after the 2 weeks.⁷⁵ This might imply that, in the cisplatin-induced CIPN model, catabolic enzymes follow a similar regulation pattern in both the CNS and PNS.

However, cannabinoid receptors exhibit distinct regulatory patterns between the CNS and PNS. In addition, another important aspect of the ECS is that it represents a fundamental system that vitally contributes to the regulation of physiological and cognitive homeostasis in our bodies, influencing various aspects such as pain, emotions, memory, and immune response.⁷⁶ Based on this, cannabinoid receptors might be regulated differently depending on the type of disease and its progression phase. In acute pathological conditions, or when there is a temporary minor disruption in homeostasis, it is suggested that endocannabinoid levels may temporarily increase to help restore normal homeostasis. However, in cases of ongoing or chronic pathological conditions, the activity of cannabinoid receptors might be increased permanently.⁷³ Taken together, this indicates that the ECS undergoes different forms of regulation depending on the specific site associated with CIPN, type of disease, and phase of development.

4. CIPN can be alleviated through TLR4 in spinal astrocytes and microglia by modulating CB1R and CB2R

Neuroinflammation is recognized as a factor influencing the onset of CIPN. Hence, efforts have been made to alleviate CIPN by targeting neuroinflammatory processes.⁷⁷⁻⁸¹ Several studies have indicated that TLR4 plays a role in regulating neuroinflammation, as well as pain associated with CIPN.^{9,82,83} The CIPN study with paclitaxel reported that activation of TLR4 by paclitaxel increased the expression of monocyte chemoattractant protein 1 (MCP-1) in DRG neurons and led to macrophage infiltration in the DRG, ultimately leading to loss of intraepidermal nerve fibers (IENF) and mechanical hypersensitivity.⁸³ Another CIPN study with paclitaxel reported that a TLR4 antagonist, LPS-RS, inhibited phosphorylation of extracellular signal related kinase 1/2 (ERK1/2) and P38, indicating TLR4 signaling via MAP kinases and NF κ B is involved in paclitaxel-induced CIPN.⁸⁴ However, previous investigations on TLR4 in CIPN were largely conducted in a paclitaxel-induced CIPN model. Therefore, it was important to investigate the regulation of TLR4 within the CIPN model induced by cisplatin. In this study, western blot analysis revealed a significant upregulation in TLR4 expression within the DRG and spinal cord in the cisplatin group. Additionally, immunohistochemistry staining was conducted to determine whether the TLR4 is expressed on glial cells. The immunohistochemistry staining results in this study showed that TLR4 co-localized with both astrocytes and microglia, but not with satellite glia cells. Several studies showed comparable outcomes through different tests.⁸⁵⁻⁸⁷ After administering the cisplatin to breast and ovarian cancer cell lines, there was a notable increase in TLR4 gene expression.⁸⁵ In addition, research on cisplatin-induced ototoxicity has reported that cisplatin activates TLR4 in a manner similar to LPS.⁸⁶ Moreover, some studies have indicated the potential activation of TLR4 by cisplatin within the CNS.^{86,87} Based on the findings of previous studies and the results of this study, it can be inferred that cisplatin increases TLR4 expression in both the CNS and PNS.

With the outcomes that cisplatin upregulated the expression of TLR4 in both the DRG

and spinal cord, our subsequent aim was to investigate the regulation of TLR4 in glial cells by administrating JZL195 and to examine its role in modulating neuroinflammation. JZL195 significantly suppressed the expression of TLR4 and reduced the expression of TNF- α and IL-1 β in the DRG and spinal cord. Also, results from immunohistochemistry staining showed that the expression of TLR4 in the DRG and spinal cord, which was increased by cisplatin, was reduced after JZL195 treatment. These findings imply that JZL195 could influence TLR4 activity in astrocytes and microglia in spinal cord, potentially affecting the modulation of neuroinflammation.

Collectively, the results of the immunohistochemistry staining indicate that JZL195 can inhibit the activity of TLR4 and possibly affect cannabinoid receptors in astrocytes and microglia. As GFAP and Iba1 co-localized with cannabinoid receptors and TLR4 in this study, TLR4 might be regulated by cannabinoid receptors in astrocytes and microglia of CNS. In contrast, cannabinoid receptors and TLR4 did not co-localize with satellite glia cells, indicating that TLR4 in the DRG is regulated by cannabinoid receptors through other cell types.

5. Antinociceptive effects of JZL195 were mediated by spinal cannabinoid receptors

In this study, JZL195 effectively alleviated two types of allodynia, which are associated with chemotherapy, by indirectly modulating cannabinoid receptors. However, the complete pharmacological mechanism of JZL195 has not been elucidated. The cannabinoid receptors are expressed in the DRG and spinal cord, both of which considered as crucial parts of the pain pathway,⁸⁸ and the present study showed that cannabinoid receptors on glial cells in the spinal cord are significantly modulated following JZL195 administration. After identifying the modulation of spinal cannabinoid receptors, the next objective of this study was to evaluate the function of spinal cannabinoid receptors in the pain modulation through JZL195 by administering AM251 and AM630 directly into the spinal fluid. As a result, inhibition of CB1R or CB2R with AM251 or AM630 led to a decrease in the

analgesic effects of JZL195 in the mechanical and cold allodynia. This indicates that the antinociceptive effects of the ECS in the CIPN animal model were mediated by the activation of spinal cannabinoid receptors.

Furthermore, distinct roles of CB1R and CB2R were observed in two types of allodynia by using different concentrations of CB1R and CB2R antagonists. The results demonstrated that the effects of JZL195 were effectively inhibited by 0.03 mg/kg of AM251 in mechanical allodynia, indicating a higher probability of CB1R contributing to the painful responses to innocuous stimuli, specifically touch, compared to CB2R. On the contrary, the results of this study suggest that both CB1R and CB2R play a role in perceiving pain elicited by non-painful cold temperatures. These results are supported by several previous studies.^{89,90} In the CIPN model, 3 mg/kg of AM251 or AM630 were administered before oxaliplatin injection.⁸⁹ Blocking CB1R using AM251 accelerated the onset of cold allodynia, while the AM630 did not affect the pain-related behavior in oxaliplatin-induced peripheral neuropathy.⁸⁹ In the study on the paclitaxel-induced CIPN model, pre-treatment with AM251 inhibited the mechanical allodynia that was relieved by 2-AG.⁹⁰ Furthermore, the antiallodynic effect produced by 2-AG was counteracted by AM630.⁹⁰ These results support the findings of the present study that AM251 and AM630 inhibit pain relief by blocking CB1R and CB2R, respectively. In another study on CIPN, AM1710, a cannabinoid receptor type 2 agonist, was utilized to inhibit the mechanical and cold allodynia induced by cisplatin. The study discovered that the antiallodynic effect was suppressed by 3 mg/kg of AM630. However, the effect of AM1710 was not hindered by 3 mg/kg of AM251.⁹¹ Collectively, the findings from this study and prior research indicate that CB1R and CB2R function differently in producing analgesia for distinct types of pain and may exert varying effects based on the administration route.

Furthermore, in the assessment of locomotor activity in normal mice, the locomotor activity of normal mice treated with JZL195 was reduced compared to untreated normal mice. This finding suggests that the pharmacological effects of JZL195 primarily occur through CB1R rather than CB2R. These experimental findings align with previous research.

Several studies have indicated that CB1R is involved in stress, fear, and anxiety circuitry, potentially contributing to the manifestation of undesired effects.^{38,92,93} In addition, a study on mood and anxiety disorders showed that inhibition of both FAAH and MAGL results in anxiety-like behavior under basal conditions.⁶⁵ However, it is premature to assert that the pharmacological effect of JZL195 in CIPN is dictated by CB1R alone, as CB2R has also been reported to play a significant role in modulating pain and neuroinflammation.^{94,95} Therefore, further studies are deemed necessary to precisely determine the pharmacological effects of JZL195.

V. CONCLUSION

In conclusion, the findings of the present study support the potential use of JZL195 in the treatment of CIPN. The inhibition of FAAH/MAGL effectively alleviated CIPN. Regulation of CB1R and CB2R through FAAH/MAGL inhibition significantly suppressed mechanical and cold allodynia in the late stage of CIPN. Additionally, JZL195 notably regulated neuroinflammation by reducing TLR4, which is an emerging neuroinflammatory factor in the development of CIPN. Furthermore, cisplatin significantly increased the expression levels of cannabinoid receptors, TLR4, GFAP, and Iba1, indicating the potential involvement of the ECS and TLR4 within astrocytes, microglia, and satellite glial cells in CIPN. Thus, the findings of this study suggest a significant role of the ECS and glial cells in alleviating pain and neuroinflammation through the use of JZL195.

REFERENCES

1. Colvin LA. Chemotherapy-induced peripheral neuropathy: Where are we now? *Pain* 2019;160 Suppl 1:S1-S10.
2. Starobova H, Vetter I. Pathophysiology of chemotherapy-induced peripheral neuropathy. *Front Mol Neurosci* 2017;10:174.
3. Jordan B, Margulies A, Cardoso F, Cavaletti G, Haugnes HS, Jahn P, et al. Systemic anticancer therapy-induced peripheral and central neurotoxicity: ESMO-EONS-EANO clinical practice guidelines for diagnosis, prevention, treatment and follow-up. *Ann Oncol* 2020;31:1306-19.
4. Burgess J, Ferdousi M, Gosal D, Boon C, Matsumoto K, Marshall A, et al. Chemotherapy-induced peripheral neuropathy: Epidemiology, pathomechanisms and treatment. *Oncol Ther* 2021;9:385-450.
5. Sisignano M, Baron R, Scholich K, Geisslinger G. Mechanism-based treatment for chemotherapy-induced peripheral neuropathic pain. *Nat Rev Neurol* 2014;10:694-707.
6. Lees JG, Makker PG, Tonkin RS, Abdulla M, Park SB, Goldstein D, et al. Immune-mediated processes implicated in chemotherapy-induced peripheral neuropathy. *Eur J Cancer* 2017;73:22-9.
7. Li T, Mizrahi D, Goldstein D, Kiernan MC, Park SB. Chemotherapy and peripheral neuropathy. *Neurol Sci* 2021;42:4109-21.
8. Fumagalli G, Monza L, Cavaletti G, Rigolio R, Meregalli C. Neuroinflammatory process involved in different preclinical models of chemotherapy-induced peripheral neuropathy. *Front Immunol* 2020;11:626687.
9. Oo TT, Pratchayasakul W, Chattipakorn N, Chattipakorn SC. Emerging roles of toll-like receptor 4 in chemotherapy-induced neurotoxicity. *Neurotoxicology* 2022;93:112-27.
10. Ji RR, Xu ZZ, Gao YJ. Emerging targets in neuroinflammation-driven chronic pain.

- Nat Rev Drug Discov 2014;13:533-48.
11. Ji RR, Chamessian A, Zhang YQ. Pain regulation by non-neuronal cells and inflammation. *Science* 2016;354:572-7.
 12. Warwick RA, Hanani M. The contribution of satellite glial cells to chemotherapy-induced neuropathic pain. *Eur J Pain* 2013;17:571-80.
 13. Di Cesare Mannelli L, Pacini A, Micheli L, Tani A, Zanardelli M, Ghelardini C. Glial role in oxaliplatin-induced neuropathic pain. *Exp Neurol* 2014;261:22-33.
 14. Agalave NM, Mody PH, Szabo-Pardi TA, Jeong HS, Burton MD. Neuroimmune consequences of eIF4E phosphorylation on chemotherapy-induced peripheral neuropathy. *Front Immunol* 2021;12:642420.
 15. Makker PG, Duffy SS, Lees JG, Perera CJ, Tonkin RS, Butovsky O, et al. Characterisation of immune and neuroinflammatory changes associated with chemotherapy-induced peripheral neuropathy. *PLoS One* 2017;12:e0170814.
 16. Wang W, Xiang P, Chew WS, Torta F, Bandla A, Lopez V, et al. Activation of sphingosine 1-phosphate receptor 2 attenuates chemotherapy-induced neuropathy. *J Biol Chem* 2020;295:1143-52.
 17. Ji RR, Donnelly CR, Nedergaard M. Astrocytes in chronic pain and itch. *Nat Rev Neurosci* 2019;20:667-85.
 18. Ji RR, Nackley A, Huh Y, Terrando N, Maixner W. Neuroinflammation and central sensitization in chronic and widespread pain. *Anesthesiology* 2018;129:343-66.
 19. Echeverry S, Shi XQ, Yang M, Huang H, Wu Y, Lorenzo LE, et al. Spinal microglia are required for long-term maintenance of neuropathic pain. *Pain* 2017;158:1792-801.
 20. Hu LY, Zhou Y, Cui WQ, Hu XM, Du LX, Mi WL, et al. Triggering receptor expressed on myeloid cells 2 (TREM2) dependent microglial activation promotes cisplatin-induced peripheral neuropathy in mice. *Brain Behav Immun* 2018;68:132-45.
 21. Leo M, Schmitt LI, Kutritz A, Kleinschnitz C, Hagenacker T. Cisplatin-induced

- activation and functional modulation of satellite glial cells lead to cytokine-mediated modulation of sensory neuron excitability. *Exp Neurol* 2021;341:113695.
22. Lee JH, Kim N, Park S, Kim SK. Analgesic effects of medicinal plants and phytochemicals on chemotherapy-induced neuropathic pain through glial modulation. *Pharmacol Res Perspect* 2021;9:e00819.
 23. Molinares D, Kurtevski S, Zhu Y. Chemotherapy-induced peripheral neuropathy: Diagnosis, agents, general clinical presentation, and treatments. *Curr Oncol Rep* 2023;25:1227-35.
 24. Acioglu C, Heary RF, Elkabes S. Roles of neuronal toll-like receptors in neuropathic pain and central nervous system injuries and diseases. *Brain Behav Immun* 2022;102:163-78.
 25. Bruno K, Woller SA, Miller YI, Yaksh TL, Wallace M, Beaton G, et al. Targeting toll-like receptor-4 (TLR4)-an emerging therapeutic target for persistent pain states. *Pain* 2018;159:1908-15.
 26. Li J, Csakai A, Jin J, Zhang F, Yin H. Therapeutic developments targeting toll-like receptor-4-mediated neuroinflammation. *Chem Med Chem* 2016;11:154-65.
 27. Buchanan MM, Hutchinson M, Watkins LR, Yin H. Toll-like receptor 4 in CNS pathologies. *J Neurochem* 2010;114:13-27.
 28. Xing F, Zhang W, Wen J, Bai L, Gu H, Li Z, et al. TLR4/NF- κ B signaling activation in plantar tissue and dorsal root ganglion involves in the development of postoperative pain. *Mol Pain* 2018;14:1744806918807050.
 29. Zhao YX, Yao MJ, Liu Q, Xin JJ, Gao JH, Yu XC. Electroacupuncture Treatment Attenuates Paclitaxel-Induced Neuropathic Pain in Rats via Inhibiting Spinal Glia and the TLR4/NF- κ B Pathway. *J Pain Res* 2020;13:239-50.
 30. Li Y, Yin C, Li X, Liu B, Wang J, Zheng X, et al. Electroacupuncture alleviates paclitaxel-induced peripheral neuropathic pain in rats via suppressing TLR4 signaling and TRPV1 upregulation in sensory neurons. *Int J Mol Sci* 2019;20.
 31. Dos Santos R, Veras F, Netto G, Elisei L, Sorgi C, Faccioli L, et al. Cannabidiol

- prevents chemotherapy-induced neuropathic pain by modulating spinal TLR4 via endocannabinoid system activation. *J Pharm Pharmacol* 2023;75:655-65.
32. Liu X, Yang W, Zhu C, Sun S, Wu S, Wang L, et al. Toll-like receptors and their role in neuropathic pain and migraine. *Mol Brain* 2022;15:73.
 33. Li Y, Zhang H, Zhang H, Kosturakis AK, Jawad AB, Dougherty PM. Toll-like receptor 4 signaling contributes to paclitaxel-induced peripheral neuropathy. *J Pain* 2014;15:712-25.
 34. Navia-Pelaez JM, Choi SH, Dos Santos Aggum Capettini L, Xia Y, Gonen A, Agatista-Boyle C, et al. Normalization of cholesterol metabolism in spinal microglia alleviates neuropathic pain. *J Exp Med* 2021;218.
 35. Cavaletti G, Marmiroli P, Renn CL, Dorsey SG, Serra MP, Quartu M, et al. Cannabinoids: An effective treatment for chemotherapy-induced peripheral neurotoxicity? *Neurotherapeutics* 2021;18:2324-36.
 36. Slivicki RA, Xu Z, Kulkarni PM, Pertwee RG, Mackie K, Thakur GA, Hohmann AG. Positive allosteric modulation of cannabinoid receptor type 1 suppresses pathological pain without producing tolerance or dependence. *Biol Psychiatry* 2018;84:722-33.
 37. Duffy SS, Hayes JP, Fiore NT, Moalem-Taylor G. The cannabinoid system and microglia in health and disease. *Neuropharmacology* 2021;190:108555.
 38. Finn DP, Haroutounian S, Hohmann AG, Krane E, Soliman N, Rice ASC. Cannabinoids, the endocannabinoid system, and pain: A review of preclinical studies. *Pain* 2021;162:S5-S25.
 39. McKenna M, McDougall JJ. Cannabinoid control of neurogenic inflammation. *Br J Pharmacol* 2020;177:4386-99.
 40. Woodhams SG, Chapman V, Finn DP, Hohmann AG, Neugebauer V. The cannabinoid system and pain. *Neuropharmacology* 2017;124:105-20.
 41. Cravatt BF, Giang DK, Mayfield SP, Boger DL, Lerner RA, Gilula NB. Molecular characterization of an enzyme that degrades neuromodulatory fatty-acid amides.

- Nature 1996;384:83-7.
42. Dinh TP, Carpenter D, Leslie FM, Freund TF, Katona I, Sensi SL, et al. Brain monoglyceride lipase participating in endocannabinoid inactivation. *Proc Natl Acad Sci U S A* 2002;99:10819-24.
 43. Silva-Cardoso GK, Lazarini-Lopes W, Hallak JE, Crippa JA, Zuardi AW, Garcia-Cairasco N, et al. Cannabidiol effectively reverses mechanical and thermal allodynia, hyperalgesia, and anxious behaviors in a neuropathic pain model: Possible role of CB1 and TRPV1 receptors. *Neuropharmacology* 2021;197:108712.
 44. Zhou Y, Xu Y, Yang J, Yu Z, Wang W, Yuan M, et al. Spinal cannabinoid receptor 2 activation alleviates neuropathic pain by regulating microglia and suppressing P2X7 receptor. *Front Mol Neurosci* 2023;16:1061220.
 45. Sheng WS, Chauhan P, Hu S, Prasad S, Lokensgard JR. Antiallodynic effects of cannabinoid receptor 2 (CB(2)R) agonists on retrovirus infection-induced neuropathic pain. *Pain Res Manag* 2019;2019:1260353.
 46. Wilkerson JL, Alberti LB, Kerwin AA, Ledent CA, Thakur GA, Makriyannis A, et al. Peripheral versus central mechanisms of the cannabinoid type 2 receptor agonist AM1710 in a mouse model of neuropathic pain. *Brain Behav* 2020;10:e01850.
 47. Long JZ, Nomura DK, Vann RE, Walentiny DM, Booker L, Jin X, et al. Dual blockade of FAAH and MAGL identifies behavioral processes regulated by endocannabinoid crosstalk in vivo. *Proc Natl Acad Sci U S A* 2009;106:20270-5.
 48. Adamson Barnes NS, Mitchell VA, Kazantzis NP, Vaughan CW. Actions of the dual FAAH/MAGL inhibitor JZL195 in a murine neuropathic pain model. *Br J Pharmacol* 2016;173:77-87.
 49. Anderson WB, Gould MJ, Torres RD, Mitchell VA, Vaughan CW. Actions of the dual FAAH/MAGL inhibitor JZL195 in a murine inflammatory pain model. *Neuropharmacology* 2014;81:224-30.
 50. Boehmerle W, Huehnchen P, Peruzzaro S, Balkaya M, Endres M. Electrophysiological, behavioral and histological characterization of paclitaxel,

- cisplatin, vincristine and bortezomib-induced neuropathy in C57Bl/6 mice. *Sci Rep* 2014;4:6370.
51. Atwal N, Winters BL, Vaughan CW. Endogenous cannabinoid modulation of restraint stress-induced analgesia in thermal nociception. *J Neurochem* 2020;152:92-102.
 52. Bajaj S, Zameer S, Jain S, Yadav V, Vohora D. Effect of the MAGL/FAAH dual inhibitor JZL-195 on streptozotocin-induced Alzheimer's disease-like sporadic dementia in mice with an emphasis on A β , HSP-70, neuroinflammation, and oxidative stress. *ACS Chem Neurosci* 2022;13:920-32.
 53. Lopes FSR, Giardini AC, Sant'Anna MB, Kimura LF, Bufalo MC, Vigerelli H, et al. Crotalphine modulates microglia M1/M2 phenotypes and induces spinal analgesia mediated by opioid-cannabinoid systems. *Int J Mol Sci* 2022;23.
 54. Ueda M, Iwasaki H, Wang S, Murata E, Poon KY, Mao J, et al. Cannabinoid receptor type 1 antagonist, AM251, attenuates mechanical allodynia and thermal hyperalgesia after burn injury. *Anesthesiology* 2014;121:1311-9.
 55. Navia-Pelaez JM, Borges Paes Lemes J, Gonzalez L, Delay L, Dos Santos Aggum Capettini L, Lu JW, et al. AIBP regulates TRPV1 activation in chemotherapy-induced peripheral neuropathy by controlling lipid raft dynamics and proximity to TLR4 in dorsal root ganglion neurons. *Pain* 2023;164:e274-e85.
 56. Woller SA, Choi SH, An EJ, Low H, Schneider DA, Ramachandran R, et al. Inhibition of neuroinflammation by AIBP: Spinal effects upon facilitated pain states. *Cell Rep* 2018;23:2667-77.
 57. Chaplan S, Pogrel J, Yaksh T. Pharmacologic modulation of tactile allodynia in a rat neuropathy model. 7th World Congress on Pain (IASP) meeting, Paris; 1993.
 58. Chaplan SR, Bach FW, Pogrel JW, Chung JM, Yaksh TL. Quantitative assessment of tactile allodynia in the rat paw. *J Neurosci Methods* 1994;53:55-63.
 59. Quasthoff S, Hartung HP. Chemotherapy-induced peripheral neuropathy. *J Neurol* 2002;249:9-17.

60. Cavaletti G, Marmiroli P. Chemotherapy-induced peripheral neurotoxicity. *Nat Rev Neurol* 2010;6:657-66.
61. Wang MS, Davis AA, Culver DG, Wang Q, Powers JC, Glass JD. Calpain inhibition protects against Taxol-induced sensory neuropathy. *Brain* 2004;127:671-9.
62. Abdollahzadeh M, Panahpour H, Ghaheri S, Saadati H. Calcitriol supplementation attenuates cisplatin-induced behavioral and cognitive impairments through up-regulation of BDNF in male rats. *Brain Res Bull* 2022;181:21-9.
63. Shabani M, Larizadeh MH, Parsania S, Hajali V, Shojaei A. Evaluation of destructive effects of exposure to cisplatin during developmental stage: No profound evidence for sex differences in impaired motor and memory performance. *Int J Neurosci* 2012;122:439-48.
64. Greco R, Demartini C, Francavilla M, Zanaboni AM, Tassorelli C. Dual inhibition of FAAH and MAGL counteracts migraine-like pain and behavior in an animal model of migraine. *Cells* 2021;10.
65. Bedse G, Bluett RJ, Patrick TA, Romness NK, Gaulden AD, Kingsley PJ, et al. Therapeutic endocannabinoid augmentation for mood and anxiety disorders: Comparative profiling of FAAH, MAGL and dual inhibitors. *Transl Psychiatry* 2018;8:92.
66. Stella B, Baratta F, Della Pepa C, Arpicco S, Gastaldi D, Dosio F. Cannabinoid formulations and delivery systems: Current and future options to treat pain. *Drugs* 2021;81:1513-57.
67. Guindon J, Lai Y, Takacs SM, Bradshaw HB, Hohmann AG. Alterations in endocannabinoid tone following chemotherapy-induced peripheral neuropathy: Effects of endocannabinoid deactivation inhibitors targeting fatty-acid amide hydrolase and monoacylglycerol lipase in comparison to reference analgesics following cisplatin treatment. *Pharmacol Res* 2013;67:94-109.
68. Illias AM, Yu KJ, Hwang SH, Solis J, Zhang H, Velasquez JF, et al. Dorsal root

- ganglion toll-like receptor 4 signaling contributes to oxaliplatin-induced peripheral neuropathy. *Pain* 2022;163:923-35.
69. Wu J, Hocevar M, Bie B, Foss JF, Naguib M. Cannabinoid type 2 receptor system modulates paclitaxel-induced microglial dysregulation and central sensitization in rats. *J Pain* 2019;20:501-14.
70. Naguib M, Xu JJ, Diaz P, Brown DL, Cogdell D, Bie B, et al. Prevention of paclitaxel-induced neuropathy through activation of the central cannabinoid type 2 receptor system. *Anesth Analg* 2012;114:1104-20.
71. Lever IJ, Robinson M, Cibelli M, Paule C, Santha P, Yee L, et al. Localization of the endocannabinoid-degrading enzyme fatty acid amide hydrolase in rat dorsal root ganglion cells and its regulation after peripheral nerve injury. *J Neurosci* 2009;29:3766-80.
72. Wilkerson JL, Gentry KR, Dengler EC, Wallace JA, Kerwin AA, Armijo LM, et al. Intrathecal cannabidiol CB(2)R agonist, AM1710, controls pathological pain and restores basal cytokine levels. *Pain* 2012;153:1091-106.
73. Di Marzo V, Petrosino S. Endocannabinoids and the regulation of their levels in health and disease. *Curr Opin Lipidol* 2007;18:129-40.
74. Ghosh K, Zhang GF, Chen H, Chen SR, Pan HL. Cannabinoid CB2 receptors are upregulated via bivalent histone modifications and control primary afferent input to the spinal cord in neuropathic pain. *J Biol Chem* 2022;298:101999.
75. Jiang F, Xia M, Zhang Y, Chang J, Cao J, Zhang Z, et al. Cannabinoid receptor-2 attenuates neuroinflammation by promoting autophagy-mediated degradation of the NLRP3 inflammasome post spinal cord injury. *Front Immunol* 2022;13:993168.
76. de Melo Reis RA, Isaac AR, Freitas HR, de Almeida MM, Schuck PF, Ferreira GC, et al. Quality of life and a surveillant endocannabinoid system. *Front Neurosci* 2021;15:747229.
77. Zhang R, Gan Y, Li J, Feng Y. Vagus nerve stimulation transiently mitigates chemotherapy-induced peripheral neuropathy in rats. *J Pain Res* 2020;13:3457-65.

78. Yang X, Jia R, Hu F, Fan W, Lin T, Zhang X, et al. Promoting AMPK/SR-A1-mediated clearance of HMGB1 attenuates chemotherapy-induced peripheral neuropathy. *Cell Commun Signal* 2023;21:99.
79. Ha JW, You MJ, Park HS, Kim JW, Kwon MS. Differential effect of LPS and paclitaxel on microglial functional phenotypes and circulating cytokines: The possible role of CX3CR1 and IL-4/10 in blocking persistent inflammation. *Arch Pharm Res* 2019;42:359-68.
80. Kim Y, Jung YH, Park SB, Kim H, Kwon JY, Kim HK, et al. TMI-1, TNF- α -converting enzyme inhibitor, protects against paclitaxel-induced neurotoxicity in the DRG neuronal cells In Vitro. *Front Pharmacol* 2022;13:842779.
81. Chen LH, Yeh YM, Chen YF, Hsu YH, Wang HH, Lin PC, et al. Targeting interleukin-20 alleviates paclitaxel-induced peripheral neuropathy. *Pain* 2020;161:1237-54.
82. Squillace S, Salvemini D. Toll-like receptor-mediated neuroinflammation: Relevance for cognitive dysfunctions. *Trends Pharmacol Sci* 2022;43:726-39.
83. Zhang H, Li Y, de Carvalho-Barbosa M, Kavelaars A, Heijnen CJ, Albrecht PJ, et al. Dorsal root ganglion infiltration by macrophages contributes to paclitaxel chemotherapy-induced peripheral neuropathy. *J Pain* 2016;17:775-86.
84. Li Y, Zhang H, Kosturakis AK, Cassidy RM, Zhang H, Kennamer-Chapman RM, et al. MAPK signaling downstream to TLR4 contributes to paclitaxel-induced peripheral neuropathy. *Brain Behav Immun* 2015;49:255-66.
85. Kashani B, Zandi Z, Karimzadeh MR, Bashash D, Nasrollahzadeh A, Ghaffari SH. Blockade of TLR4 using TAK-242 (resatorvid) enhances anti-cancer effects of chemotherapeutic agents: A novel synergistic approach for breast and ovarian cancers. *Immunol Res* 2019;67:505-16.
86. Babolmorad G, Latif A, Domingo IK, Pollock NM, Delyea C, Rieger AM, et al. Toll-like receptor 4 is activated by platinum and contributes to cisplatin-induced ototoxicity. *EMBO Rep* 2021;22:e51280.

87. Squillace S, Niehoff ML, Doyle TM, Green M, Esposito E, Cuzzocrea S, et al. Sphingosine-1-phosphate receptor 1 activation in the central nervous system drives cisplatin-induced cognitive impairment. *J Clin Invest* 2022;132.
88. Pertwee RG. Cannabinoid receptors and pain. *Prog Neurobiol* 2001;63:569-611.
89. Pereira AF, Lisboa MRP, de Freitas Alves BW, da Silva CMP, Dias DBS, de Menezes KLS, et al. Endocannabinoid system attenuates oxaliplatin-induced peripheral sensory neuropathy through the activation of CB1 receptors. *Neurotox Res* 2021;39:1782-99.
90. Thomas A, Okine BN, Finn DP, Masocha W. Peripheral deficiency and antiallodynic effects of 2-arachidonoyl glycerol in a mouse model of paclitaxel-induced neuropathic pain. *Biomed Pharmacother* 2020;129:110456.
91. Deng L, Guindon J, Vemuri VK, Thakur GA, White FA, Makriyannis A, et al. The maintenance of cisplatin- and paclitaxel-induced mechanical and cold allodynia is suppressed by cannabinoid CB₂ receptor activation and independent of CXCR4 signaling in models of chemotherapy-induced peripheral neuropathy. *Mol Pain* 2012;8:71.
92. Almeida MM, Dias-Rocha CP, Calviño C, Trevenzoli IH. Lipid endocannabinoids in energy metabolism, stress and developmental programming. *Mol Cell Endocrinol* 2022;542:111522.
93. Gunduz-Cinar O. The endocannabinoid system in the amygdala and modulation of fear. *Prog Neuropsychopharmacol Biol Psychiatry* 2021;105:110116.
94. Dos Santos RS, Veras FP, Netto GP, Sorgi CA, Faccioli LH, Vilela LR, et al. Cannabidiol reduces lipopolysaccharide-induced nociception via endocannabinoid system activation. *Basic Clin Pharmacol Toxicol* 2023;133:16-28.
95. Sun L, Dong R, Xu X, Yang X, Peng M. Activation of cannabinoid receptor type 2 attenuates surgery-induced cognitive impairment in mice through anti-inflammatory activity. *J Neuroinflammation* 2017;14:138.

ABSTRACT (IN KOREAN)

**항암화학요법으로 유발된 말초신경병증에서 교세포와
내인성 카나비노이드 시스템을 통한 JZL195의 통증 조절 기전 규명**

< 지도교수 이 배 환 >

연세대학교 대학원 의과학과

김 리 정

항암화학요법으로 유발된 말초신경병증(chemotherapy-induced peripheral neuropathy, CIPN)은 항암화학요법을 받은 후 나타나는 가장 심각한 부작용 중 하나이다. CIPN의 병태생리는 복잡하고 다원적이며, 따라서 그 발병 기전은 사용하는 화학요법의 종류에 따라 달라진다. 이러한 이유로 인해 CIPN과 관련된 증상을 감소시키는 것이 CIPN을 겪는 환자들의 삶의 질을 향상하기 위한 최적의 방안으로 알려져 있다. 그러나 CIPN의 발생 및 치료와 관련된 명확한 메커니즘이 아직까지 밝혀지지 않았기에 이 또한 어려움을 겪고 있다. 따라서 본 연구는 지방산 아마이드(fatty acid amide hydrolase, FAAH)와 모노아실글리세롤(monoacylglycerol lipase, MAGL)을 동시에 억제하는 JZL195를 사용하여 신경교세포에 발현하고 있는 카나비노이드 수용체(cannabinoid receptor)를 조절함으로써 CIPN을 완화하고, 신경교세포(glial cell)와 내인성 카나비노이드 시스템

(endocannabinoid system) 사이의 연관성을 밝히고자 했다.

본 연구에서는 시스플라틴(cisplatin)을 사용해 CIPN 동물 모델을 형성하고 JZL195를 세 가지 농도로 투여한 후 행동 검사를 통해 기계적 이질통(mechanical allodynia) 및 냉각 이질통(cold allodynia)을 측정하였다. 이후 웨스턴 블롯 분석을 통해 척수 및 척수신경절에서 FAAH, MAGL, CB1R, CB2R의 발현양을 확인하였고 추가적으로 TLR4와 염증성 인자들의 발현양을 신경교세포와 함께 확인하였다. 또한, 척수와 척수신경절에서 유의한 변화를 보인 CB1R, CB2R, TLR4가 신경교세포 내에서 조절되는지 확인하기 위해 면역조직화학염색을 수행했다. 행동검사 결과, 20 mg/kg의 JZL195가 두 종류의 이질통을 모두 유의미하게 완화시킴을 확인하였고, 웨스턴 블롯 결과를 통해 FAAH, MAGL, cannabinoid receptor 1/2 (CB1/2R)의 발현양이 조절되는 것을 확인하였다. 또한, 웨스턴 블롯을 통해 CIPN의 발병 기전 중 하나로 떠오르는 신경염증(neuroinflammation)에 중요한 역할을 하는 톨유사수용체 4 (toll-like receptor 4, TLR4)의 발현양과 TNF- α , IL-1 β 의 발현양이 JZL195에 의해 감소됨을 발견하였다. 이와 더불어 척수의 성상세포(astrocytes) 및 미세아교세포(microglia)와 척수신경절의 위성 신경교세포(satellite glial cell)가 시스플라틴에 의해 활성화 되었다가 JZL195에 의해 억제됨을 확인하였다. 면역조직화학염색을 통해 신경교세포의 형태학적 변화와 CB1R, CB2R, TLR4의 발현 변화를 관찰함과 동시에 이들이 성상세포 및 미세아교세포와 함께 염색된 것을 확인하였으나 위성 신경교 세포와는 함께 염색되지 않은 것을 알 수 있었다.

본 연구의 결과들을 통해 JZL195를 사용하여 FAAH/MAGL을 억제하면 CIPN을 효과적으로 완화할 수 있으며, 이러한 CIPN 완화 효과는 신경교세포의 활성화와 카나비노이드 수용체가 밀접한 작용을 통해 나타나는 것임을 시사한다.

핵심되는 말: 항암화학요법에 의한 말초신경병증, 내인성 카나비노이드 시스템, 신경교세포, 신경염증, 톨유사수용체 4